

Aus der Kooperationseinheit Dermatoonkologie,
Deutsches Krebsforschungszentrum (DKFZ), Heidelberg
(Abteilungsleiter: Prof. Dr. med. Jochen Sven Utikal)
und
Klinik für Dermatologie, Venerologie und Allergologie,
Universitätsklinikum Mannheim, Ruprecht-Karls-Universität Heidelberg
(Klinikdirektor: Prof. Dr. med. Sergij Goerd)

STAT3 – the switch of melanoma-associated NRAS mutations

Inauguraldissertation
zur Erlangung des medizinischen Doktorgrades
der
Medizinischen Fakultät Mannheim
der Ruprecht-Karls-Universität
zu
Heidelberg

vorgelegt von
James Kim

aus
Heidelberg

2020

Dekan: Prof. Dr. med. Sergij Goerd

Doktorvater: Prof. Dr. med. Jochen Sven Utikal

Parts of this work have been published in

Poster Presentations

Kim, J., Larribere, L., Novak, D. & Utikal, J. Influence of melanoma-associated NRAS mutations. *Deutscher Hautkrebskongress* (Mainz, Germany). 2017

Kim, J., Larribere, L., Novak, D. & Utikal, J. Influence of melanoma-associated NRAS mutations. *Hallmarks of Skin Cancer Conference* (Heidelberg, Germany). 2017

Publications

Kim, J., Novak, D., Sachpekidis, C., Utikal, J. & Larribère, L. STAT3 Relays a Differential Response to Melanoma-Associated NRAS Mutations. *Cancers (Basel)*. **12**, 119 (2020).

TABLE OF CONTENTS

	Page
ABBREVIATIONS	1
1 INTRODUCTION.....	7
1.1 Malignant Melanoma: Epidemiology.....	7
1.2 Malignant Melanoma: Etiology	7
1.3 Malignant Melanoma: Diagnostics.....	8
1.4 Malignant Melanoma: Therapeutic Strategies	9
1.5 NRAS Mutations	11
1.5.1 The Genetic Landscape of Melanoma	11
1.5.2 The MAPK-Pathway	12
1.5.3 NRAS Mutational Status in Melanoma	14
1.5.4 Clinical Characteristics of NRAS Mutant Melanoma.....	15
1.5.5 <i>NRAS</i> and Resistance Mechanisms	15
1.6 Oncogene-Induced-Senescence	16
1.7 The Role of STAT3	18
1.8 Aim of the Thesis	19
2 MATERIAL AND METHODS.....	20
2.1 Materials	20
2.1.1 Reagents and Kits.....	20
2.1.2 Reagents for Cell Culture.....	22
2.1.3 Human Cell Lines.....	23
2.1.4 Antibodies.....	23
2.1.5 Plasmids.....	24

2.1.6	siRNA	24
2.1.7	Primers	25
2.1.8	Solutions and Buffers.....	25
2.2	Equipment.....	27
2.2.1	Software Tools	28
2.3	Methods	29
2.3.1	Cell Culture	29
2.3.2	Lentiviral Transduction.....	29
2.3.3	siRNA	30
2.3.4	Senescence Quantification	31
2.3.5	RNA Isolation.....	31
2.3.6	cDNA Synthesis.....	31
2.3.7	Quantitative Real-time PCR.....	32
2.3.8	Protein Isolation.....	32
2.3.9	Western Blot.....	33
2.3.10	Whole Genome Microarray Analysis	33
2.3.11	Proliferation	34
2.3.12	Colony Formation.....	34
2.3.13	Migration.....	34
2.3.14	Proteome Profiler Array	35
2.3.15	Statistical Analyses.....	35
3	RESULTS	36
3.1	<i>NRAS</i> ^{G12/13} mutants induce a stronger OIS-associated phenotype than <i>NRAS</i> ^{Q61} mutants in normal human melanocytes.....	36
3.2	<i>NRAS</i> ^{Q61K} expression induces a distinct secretory phenotype, tyrosine kinase activation and gene expression compared to <i>NRAS</i> ^{G12V} in NHM	39
3.3	The STAT3 Pathway is differentially activated by <i>NRAS</i> ^{Q61} and <i>NRAS</i> ^{G12/13} in NHM.....	41

3.4	<i>NRAS</i> ^{Q61H} increases proliferation, migration and colony formation of immortalized melanocytes MelSTV greater than <i>NRAS</i> ^{G12V} and associates with STAT3 activation	44
3.5	Upregulation of <i>MMP2</i> , <i>IL-1β</i> and <i>IL1R</i> is STAT3 mediated	48
3.6	<i>NRAS</i> ^{Q61H} shows increased tumorigenesis in melanoma cell lines.....	50
4	DISCUSSION	51
4.1	<i>NRAS</i> ^{Q61} shows a more tumorigenic phenotype than <i>NRAS</i> ^{G12/13}	51
4.2	STAT3 as a driver in <i>NRAS</i> -mediated melanomagenesis.....	52
4.2.1	STAT3 in normal human melanocytes.....	54
4.2.2	STAT3 in immortalized melanocytes.....	57
4.2.3	STAT3 inhibition as a new therapeutic option in <i>NRAS</i> mutant melanoma.....	59
5	CONCLUSION.....	60
6	REFERENCES	61
7	SUPPLEMENTARY FIGURES AND TABLES	72
7.1	Supplementary Figures	72
7.2	Supplementary Tables	74
7.2.1	Supplementary Table 1	74
8	CURRICULUM VITAE.....	76
9	ACKNOWLEDGEMENTS	77

ABBREVIATIONS

$\Delta\Delta CT$	Delta delta cycle threshold
%	Percent
°C	Degrees Celsius
AKT	Protein kinase B
ASO	Antisense oligonucleotide
ATM	Ataxia-telangiectasia mutated
ATR	Ataxia telangiectasia and Rad3 related
BCA	Bicinchoninic acid assay
BCL2	B-cell lymphoma 2
BEX1	Brain-expressed X-linked protein 1
BRAF	v-Raf murine sarcoma viral oncogene homolog B
BRAFi	BRAF-inhibitor
BSA	Bovine serum albumin
c-myc	MYC Proto-Oncogene
CDK4	Cyclin-dependent kinase 4
CDKN2A	Cyclin-dependent kinase Inhibitor 2A
cDNA	Complementary DNA
CTLA-4	Cytotoxic T lymphocyte antigen-4
Ctrl	Control
DAPI	4',6-diamidino-2-phenylindole
dbcAMP	Dibutyl cyclic adenosine monophosphate

DDR	DNA-damage-repair
dH ₂ O	Distilled water
DKFZ	Deutsches Krebsforschungszentrum
DMSO	Dimethyl sulfoxide
DNA	Deoxyribonucleic acid
DNA-PK	DNA-dependent protein kinase
DNA-SCARS	DNA segments with chromatin alterations reinforcing senescence
dNTP	Deoxyribose nucleoside triphosphate
e.g.	Exempli gratia
EDTA	Ethylenediaminetetraacetic acid
EF1 α	Elongation factor 1-alpha
ELISA	Enzyme-linked Immunosorbent Assay
EMT	Epithelial–mesenchymal transition
Eph	Ephrin
ERK	Extracellular signal-regulated kinases
et al.	Et alii
etc.	Et cetera
FACS	Fluorescence-activated cell sorting
FCS	Fetal calf serum
FDA	Food and Drug Administration
g	Grams
G-CSF	Granulocyte-colony stimulating factor

G-protein	Guanine nucleotide-binding proteins
GAP	GTPase activating protein
GDP	Guanosine diphosphate
GEF	Guanine-nucleotide exchange factor
GNA11	Guanine nucleotide-binding protein subunit alpha-11
GNAQ	Guanine nucleotide-binding protein G(q)
GTP	Guanosine-5'-triphosphate
HRAS	Harvey rat sarcoma
HRP	Horseradish peroxidase
hTERT	Telomerase holoenzyme
IBMX	3-Isobutyl-1-methylxanthine
IFN	Interferon
IgG	Immunoglobulin G
IL	Interleukin
IRES	Internal ribosome entry site
KRAS	Kirsten rat sarcoma
l	Liter
LB	Lysogeny broth
MAPK	Mitogen-activated protein kinase
MEKi	MEK-inhibitor
mg	Milligrams
min	Minute

MITF	Microphthalmia-associated transcription factor
ml	Milliliter
mM	Millimolar
mm	Millimeters
MMP	Matrix metalloproteinase
MRI	Magnetic resonance imaging
mRNA	Messenger ribonucleic acid
Na ₃ VO ₄	Sodium Orthovanadate
NF1	Neurofibromin 1
ng	Nanograms
NHM	Normal human melanocyte
nl	Non infected
nm	Nanometers
NRAS	Neuroblastoma rat sarcoma
NSG	NOD scid gamma
OIS	Oncogene-induced senescence
oligoDT	Oligo 15–25 Desoxythymidine
ORR	Objective response rate
OS	Overall survival
PAI-1	Plasminogen activator inhibitor-1
PBS	Phosphate-buffered saline
PD-1	Programmed cell death-1

PD-L1	Programmed cell death-1 ligand
PDGF	Platelet-derived growth factor
PET-CT	Positron emission tomography–computed tomography
PFS	Progression free survival
PI3K	Phosphoinositide 3-kinase
pmol	Picomolar
PREX2	Phosphatidylinositol-3,4,5-trisphosphate-dependent Rac exchange factor 2
PVDF	Polyvinylidene difluoride
qPCR	Quantitative polymerase chain reaction
RAS	Rat sarcoma
Rb	Retinoblastoma
RNA	Ribonucleic acid
ROS	Reactive oxygen species
RTK	Receptor tyrosine kinase
SA- β -Gal	Senescence-associated- β -Galactosidase activity
SAHF	Senescence-associated heterochromatin foci
SASP	Senescence-associated secretory phenotype
SDS-PAGE	Sodium dodecyl sulfate polyacrylamide gel electrophoresis
shRNA	Short hairpin RNA
siRNA	Small interfering RNA
siSCR	Small interfering scrambled RNA
SMS	Senescence-messaging secretome

STAT3	Signal Transducer and Activator of Transcription 3
STC1	Stanniocalcin-1
SV40ER	Simian Virus 40 early region
TAGLN3	Transgelin-3
TBS	Tris-buffered saline
TEMED	Tetramethylethylenediamine
TERT	Telomerase reverse transcriptase
TGF- β	Transforming growth factor beta
U	Units
US	United States
UV	Ultraviolet
UVR	Ultraviolet radiation
VEGF	Vascular Endothelial Growth Factor
vs.	Versus
WNT	Wingless-related integration site
WT	Wildtype
μm	Micrometer
μM	Micromolar

1 INTRODUCTION

1.1 Malignant Melanoma: Epidemiology

In 2018, about 31 400 new cases and around 3 600 deaths were reported to be caused by melanoma in Germany¹. Although melanoma is not the most common cancer, it is by far the deadliest of skin cancers because of its very early and aggressive formation of metastasis. The 5-year survival rate of patients with metastatic melanoma is only 25%². Melanoma arises most frequently on the skin originating from melanocytes but can be also found as uveal, mucosal or very rarely as meningeal melanoma^{3,4}.

The incidence of melanoma is rising around the globe. Its highest incidence (new cases per 100.000) can be found in Australia and New Zealand, together with 145.9, respectively, compared to North America with 54.6, Central and Eastern Europe with 5.9 and Eastern Asia with 1.2¹. Both sexes are similarly affected. The differences in incidence can be partially explained by exposure to risk factors such as ultraviolet radiation, but there are multiple other factors contributing to different distribution of melanoma incidence which are explained in detail below.

1.2 Malignant Melanoma: Etiology

The etiopathogenesis of melanoma is heterogeneous and results from different environmental and internal, mostly genetic, risk factors. Important risk factors include family history of melanoma, multiple benign or atypical nevi, and previous history of melanoma⁵. Additional factors, such as immunosuppression, sun sensitivity and exposure to ultraviolet radiation increase the risk of melanoma.

Positive family history is an independent internal risk factor for melanoma as hereditary melanoma accounts for around 10% of cutaneous melanoma⁶. Especially germline mutations in *CDKN2A*, which encodes two tumor suppressor genes *p16INK4A* and

p19ARF, are responsible for around 40% of this subgroup^{5,7,8}. Another gene affected is *CDK4*. However, the vast majority of melanoma originates from sporadic mutations.

These sporadic mutations are caused by ultraviolet radiation (UVR), another important risk factor. UVR affects the genome through direct and indirect genetic changes^{9,10}. Direct damage of the DNA is mostly caused by UV-B radiation (280–320), whereas UV-A (320–400 nm) seems to harm the DNA more indirectly by producing reactive oxygen species (ROS) and suppressing the immune system¹¹. UV-C (100–280 nm) is blocked by ozone and therefore plays a minor role in melanomagenesis.

Especially when DNA repair mechanisms are altered, the affected melanocyte is prone to additional mutations and therefore to protumorigenic changes¹². Of note, not regular chronic sun exposure, but in particular irregular and intense exposure to sunlight in young ages, was significantly associated with increased risk of melanoma^{13–15}. Equally important to environmental factors are host factors for sun susceptibility, such as fair skin and hair color, as well as red hair color. The number of freckles and nevi is an additional risk factors for melanoma^{16,17}.

1.3 Malignant Melanoma: Diagnostics

Taking the aggressive spread of melanoma into account, early diagnosis and treatment in early stages are essential for successful eradication of melanoma. The different pillars of diagnostics are primarily built on the clinical diagnosis which considers the phenotype and thorough history taking of risk factors. Suspicious skin lesions can be evaluated by presentation of symmetry, irregularity of borders, pigmentation and color, diameter and elevation. But as melanoma arises in different phenotypes, including an atypical presentation as amelanotic melanoma, diagnosis can be difficult. An accurate and safe diagnosis of clear and unclear lesions can be made through excisional biopsy followed by histopathological analysis, which then results in the resection of safety margins depending on the histology. Staging examinations with inspection and examination of

the whole integument including the lymph node status is inevitable. Moreover, the assessment of tumor markers, such as S100B, (PET-) computed tomography (CT) scan or magnetic resonance imaging (MRI), mutational analysis of *BRAF* and the sentinel biopsy can complete the stage-adapted diagnostics¹⁸. Still, the evaluation of the *NRAS* mutational status is not yet a standard procedure. The importance of the mutational status in melanoma and its therapy will be discussed later.

The prognosis of melanoma patients is mostly determined by tumor thickness before resection^{19,20}. A prognostic classification has been developed according to the invasion into the skin layers (Breslow Index) and has an almost linear correlation to the statistically expected 10-year survival rate.

1.4 Malignant Melanoma: Therapeutic Strategies

The essential therapy concept is still the R0-resection of the tumor with a defined safety margin depending on the tumor thickness^{18,20}. Solitary metastasis can be treated locally. Advanced stage diseases have a bad prognosis due to dissemination and distant metastasis. However, new systemic therapeutic approaches and targeted therapies have significantly improved the survival of these patients over the last 10 years and are still evolving.

Especially *BRAF* mutated melanoma has efficient treatment options with *BRAF*-inhibitors (Vemurafenib, Dabrafenib and Encorafenib) in combination with MEK-inhibitors (Cobimetinib, Trametinib and Binimetinib) or immune checkpoint inhibitors (Ipilimumab, Nivolumab, Pembrolizumab).

Attempts treating *NRAS* mutated melanoma are still sobering as *NRAS* is still thought to be an “undruggable” target due to missing effective *NRAS* inhibiting agents^{21–26}. Initial efforts to target *NRAS* itself or related posttranslational modifications with farnesyl transferase inhibitors have been unsuccessful, accompanied by many adverse reactions and low response rates^{27,28}.

However, current research is widening the initial focus away from the tumor cell itself. Great interest has been given to the tumor environment and the cell-cell-interaction through a secretion of cytokines and immunological effects of melanoma cells. Immune therapies have evolved in the field of melanoma and show effects as an effective non-mutation-specific therapy²⁹. It is the first-line therapy, especially in *BRAF* wildtype melanoma. IL-2 was introduced early in the treatment of metastatic melanoma, showing a decent effect but with severe adverse effects³⁰. So called 'immune checkpoint inhibitors' are therefore gaining increasing interest as they promote the endogenous antitumor immunity. Firstly introduced, Ipililumab, a monoclonal antibody directed at cytotoxic T lymphocyte antigen-4 (CTLA-4), increased the survival in metastatic melanoma.^{31,32} It was then soon followed by Nivolumab and Pembrolizumab, another class of immune therapeutics, both targeting the programmed cell death-1/ligand (PD-1/PD-L1). In a clinical randomized phase III trial Nivolumab presented an increased (ORR 27% vs. 10%) and durable response rate compared to chemotherapy (median duration of response 32 months vs. 13 months), but without overall survival benefit³³.

Furthermore, Nivolumab combined with Ipililumab or Nivolumab alone were superior to Ipililumab therapy regarding PFS (Nivolumab + Ipililumab 11.5 month vs. Ipililumab alone 2.9 month vs. Nivolumab alone 6.9 month), OS benefit (52% vs. 26% vs. 44%) and greater ORR (59% vs. 21% vs. 74%)^{34,35}.

Similarly, Pembrolizumab showed a benefit over conventional chemotherapy and Ipililumab therapy in randomized clinical trials³⁶. It is also FDA approved for advanced unresectable, metastatic melanoma or as an adjuvant treatment for stage III melanoma after complete resection.

Whether *NRAS*-mutant melanoma in particular benefits from immunotherapy is still under investigation and needs prospective trials as recent literature is based on retrospective data. In a retrospective cohort of *NRAS* melanoma receiving immunotherapy (IL2, Ipilimumab or Anti-PD-1/PD-L1), Johnson et al. showed a trend to better outcomes including response rates, clinical benefit and progression-free survival

compared to *BRAF* or *NRAS/NRASWT*³⁷. In contrast, another retrospective study stated similar responses to immunotherapy independent of *NRAS* mutational status³⁸.

An ongoing phase III trial (NEMO) comparing the MEK-inhibitor Binimetinib to Dacarbazine therapy on *NRAS*-mutated patients showed promising results with an increased median progression-free survival of 2.8 months (95% CI 2.8–3.6) in the Binimetinib group compared to 1.5 months (1.5–1.7) in the Dacarbazine group (hazard ratio 0.62 [95% CI 0.47–0.80]; one-sided $p < 0.001$) but not in overall survival³⁹. Recently, a preclinical study has described a new combination strategy involving BET inhibitors with MEK inhibitors to overcome drug resistance (**see 1.5.5**) in *NRAS*-mutant melanoma and to improve efficiency⁴⁰. In addition to MEK-inhibitors, other targets such as BCL2, TERT and different kinases are being tested as combination partners to treat *NRAS* mutant melanoma^{41–44}.

As immunotherapies and MEK-inhibitors show partial response rates, additional targets in combination might be helpful to fight *NRAS*-mutated melanoma.

1.5 NRAS Mutations

1.5.1 The Genetic Landscape of Melanoma

Having a look at the mutational status, malignant melanoma harbors the most genetic mutations compared to other cancer types⁴⁵. Common mutations can be detected in the MAPK pathway. The oncogene *BRAF* is the mostly affected gene (52%), followed by mutations in the *NRAS* gene (28%), in *TP53* (15%), *NF1* (14%) and *CDKN2A* (13%)^{46,47} (Figure 1).

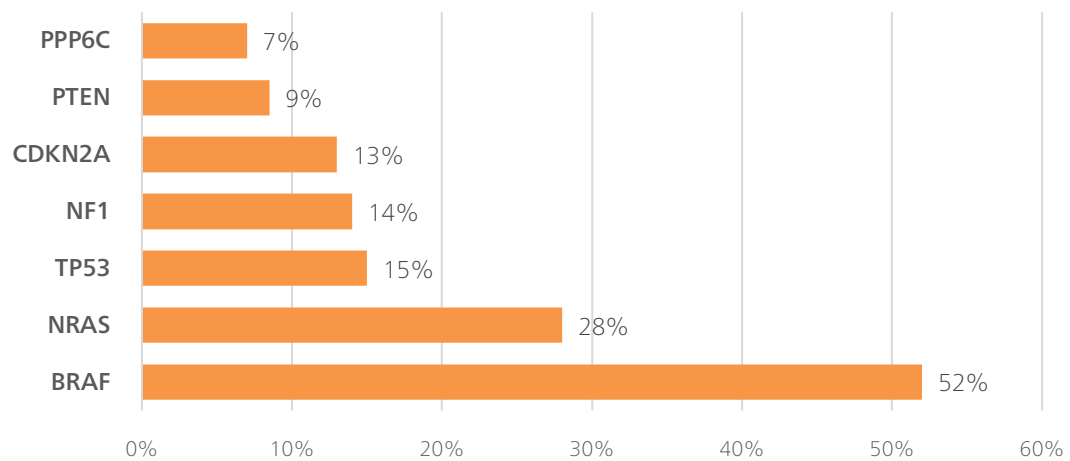


Figure 1 | Landscape of driver mutations in melanoma

Frequency of driver mutations in melanoma by whole genome sequencing data n=318. Adapted from Akbani et al.⁴⁷

1.5.2 The MAPK-Pathway

The MAPK-Pathway activates a cascade of kinases (RAS, RAF, MEK and ERK) and its tight regulation is important for cell function.

The RAS (Rat sarcoma) family consists of small G-proteins which function as molecular switches controlling downstream signaling pathways and influencing cellular proliferation, differentiation and survival (**Figure 2**)⁴⁸. There are three isoforms, *HRAS*, *KRAS* and *NRAS*, which are commonly mutated in one third of human cancer types. *KRAS* is found mutated most frequently (>20%), followed by *NRAS* (8.5%) and *HRAS* (3.3%)⁴⁹. Of these isoforms *NRAS* is specifically affected in melanoma.

RAS proteins can be found in a GTP-bound active state and GDP-bound inactive state. Regulation towards the active state is promoted by GEF (guanine-nucleotide exchange factor) which replaces GDP with GTP. In contrast, GAPs (GTPase activating protein) drive the hydrolysis of GTP into GDP, inactivating RAS.

Activated RAS binds and activates the kinase RAF which then leads to a change in conformation and dimerization. Activated RAF in turns phosphorylates the MEK-kinase. The ERK-kinase then effects a set of transcription factors.

MAPK signaling is not the only pathway affected, but there are other pathways deregulated, such as the PI3K-AKT-signalling, WNT-signaling and EMT-associated signalling⁵⁰⁻⁵². The role of other pathways and targets for therapies is still under investigation and is crucial to fully understand melanoma initiation and progression.

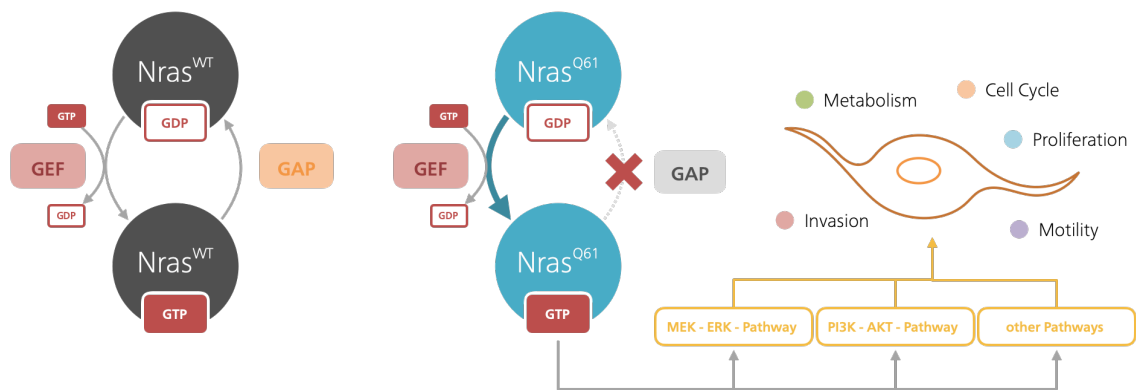


Figure 2 | Mutation in the NRAS gene leads to continuous activation of downstream signaling pathways

A In the normal state NRAS is a small GTPase hydrolyzing GTP into GDP. GTP-bound NRAS forms the active complex activating downstream effectors. GDP-bound NRAS is inactive. Additional factors such as GEF (guanine-nucleotide exchange factor) and GAPs (GTPase activating protein) regulate the activation of NRAS. GEF replaces GDP with GTP and activates NRAS. In contrast, GAP promotes the hydrolysis of GTP into GDP and therefore inactivates the NRAS protein. **B** When the NRAS gene is mutated (e.g. in codon 61) a continuously active NRAS protein leads to constant activation of the main downstream pathways MEK-ERK and PI3K-AKT and alters proliferation, cell cycle, metabolism invasion and motility of the cell.

1.5.3 NRAS Mutational Status in Melanoma

Mutations in the *NRAS* gene are not equally distributed. In fact, somatic mutations in cutaneous melanoma can be almost exclusively found in codon 61 (93%) rather than in codon 12 or 13 (5%), although they all possess an oncogenic activity^{46,53}. Interestingly, *NRAS* mutations show a more equally distributed frequency of codon 12 or 13 mutations (46%) compared to codon 61 mutations (54%) in mucosal melanoma⁵⁴. The authors discuss a possible involvement of preferable UV-induced genesis of *NRAS*Q61 mutations in cutaneous melanoma compared to non-UV-exposed mucosal melanoma where other carcinogens may play a leading role. Even though considerable research has been devoted unveiling the characteristics of *NRAS* mutant melanoma, rather less attention has been paid to these distributional differences in codon mutations. However, these differences of position and type of substitution are not fully understood yet but can be seen throughout different cancer types. Different factors are discussed to contribute to the diversity of patterns among *RAS* mutated cancers, such as structural differences, additional regulating proteins, localization, signaling intensity, cell-specific response and also microenvironmental differences^{53,55}. Nevertheless, they surely have clinical implications as different codon mutations affect the tumor's aggressiveness or response to therapy. In non-small-cell lung cancer *KRAS*12 mutations are associated with lower progression free survival compared to other *RAS* mutations⁵⁶. Therapy response to Cetuximab in colon cancer is reduced if the tumor harbors a *KRAS*12 mutation, whereas *KRAS*13 responds well⁵⁷. In fact, in melanoma *NRAS*Q61 was described to induce greater tumor formation than *NRAS*G12 in a melanoma mouse model, but the underlying mechanisms are not fully understood so far. Differences in biochemical behavior have been suggested with higher affinity of GTP binding, increased stability and reduced intrinsic GTPase activity of codon 61 mutated *NRAS* melanoma⁵⁸. Whether a differential activation of downstream molecular pathways contribute to these differences, remains yet unclear.

1.5.4 Clinical Characteristics of NRAS Mutant Melanoma

NRAS mutational status in melanoma is not only of scientific interest but is an independent negative prognostic factor when compared to *NRAS* wildtype and *BRAF* mutated melanoma⁵⁹. It has a higher mitotic activity, forms thicker tumors and is associated with shorter melanoma-specific survival⁶⁰. Furthermore, in stage four metastatic melanoma, *NRAS* mutated melanoma showed a decreased overall survival when compared to *NRAS* wildtype melanoma (median survival 8.2 month vs. 15.1 months, $p=0.004$)⁵⁹. In this study, the formation of brain metastasis was also seen increased when comparing to *NRAS* WT melanoma.

Whereas *BRAFV600E* mutant melanoma arises mostly in intermittent-UV-exposed skin, *NRAS* mutational status is associated with chronic sun exposure and high mutational burden^{44,60}. A trend has been shown that UVR leads to more *NRASQ61* mutations rather than *NRASG12/13* mutations, preferentially targeting pyrimidine dimers⁶¹.

Taken together, *NRAS* mutant melanoma shows worse clinical characteristics and it remains of great interest to improve the treatment of this special subgroup of melanoma patients.

1.5.5 NRAS and Resistance Mechanisms

Treatment with BRAF-inhibitors (BRAFi) shows good initial tumor response but is limited as it recurs approximately one year after treatment due to resistance mechanisms. The importance to understand *NRAS* mutant melanoma is of further interest, as acquired resistance in BRAFi-treated melanoma shows secondary *NRAS* mutations to escape drug therapy among other mechanisms. Secondary *NRAS* mutations were associated with brain metastasis and Vemurafenib use²³. Focusing on different codon mutations, 85% occurred in *NRASQ61*, but only 15% in *NRASG12*. Our study might help to also overcome secondary *NRAS* mutational resistance.

1.6 Oncogene-Induced-Senescence

Replicative senescence is a physiological process of cells in the human body which hinders old damage-acquired cells to proliferate after telomere shortening with the life span of this cell^{62,63}. However, a broader understanding of senescence has been reached as another mechanism of cell arrest has been found. Mutations in oncogenes, such as in *RAS* proteins, were discovered to also induce a prolonged and irreversible arrest in primary mammalian cells, so called oncogene-induced senescence (OIS) as a mechanism of tumor suppression^{64–66}. Recently, Gorgoulis et al. defined four hallmarks of senescence which are (1) cell cycle withdrawal, (2) macromolecular damage, (3) secretory phenotype and (4) deregulated metabolism (**Figure 3**)⁶⁷. These hallmarks demonstrate that oncogenes induce a substantial change in intrinsic mechanisms of the cell.

The first mechanism is the cell's response to repress the expression of genes involved in proliferation. Accordingly, the expression of an oncogene in primary cells is followed by alterations in the chromatin structure forming senescence-associated heterochromatin foci (SAHF). These changes are caused by histone modifications⁶⁸. In addition to SAHF-formation, oncogene-induced senescence promotes the formation of senescence-associated DNA damage foci, so called DNA-SCARs (DNA segments with chromatin alterations reinforcing senescence) and activates DNA-damage-repair (DDR) mechanisms mediated by ATM, ATR, DNA-PK and p53^{68–70}. Upon DDR activation cell cycle arrest, DNA repair and replication restart are initiated. The OIS cell program is further mediated through cytostatic INK4A–retinoblastoma (Rb) and ARF–p53 signaling cascades which finally again promotes cell cycle arrest.

Beside oncogenes, exposure to cytokines such as INF- β or TGF- β are also able to induce OIS in cells^{71–73}. That's why special interest has been given to secreted factors of senescent cells. Subsequently, a specific secretome of senescent cells has been described, including proinflammatory cytokines and chemokines, angiogenic factors, growth modulators, and matrix metalloproteinases (MMPs) (e.g. IL-6, IL-1 α , IL-1 β , IL-8, G-CSF, IFN- γ , PAI-1, etc.)^{74,75}. Also known as senescence-associated secretory phenotype

(SASP) or senescence-messaging secretome (SMS), it affects the microenvironment. It therefore promotes inflammation through paracrine effects on fibroblasts which further sensitize neighboring cells to senesce or inhibit proliferative signals from the environment. The fact that tumor cells in later stages misuse this secretome to promote tumor progression shows the pleiotropic role of the secreted factors.

These powerful mechanisms in reaction to oncogenes display potent internal tumor suppressing mechanisms. Therefore, cooperating genetic alterations are needed to override OIS in primary cells and induce tumor formation⁷⁶. However, oncogenic *RAS* can transform immortalized rodent cells as they already carry additional alterations⁷⁷.

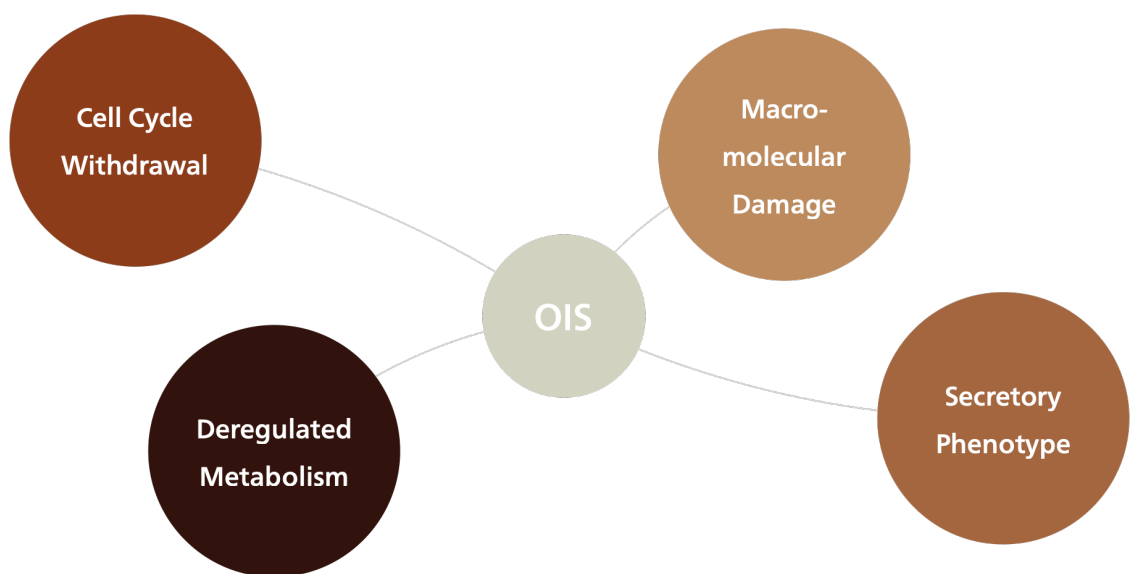


Figure 3 | Hallmarks of Oncogene-Induced Senescence

Cells undergoing oncogene-induced senescence present the following four hallmarks: macromolecular damage, a secretory phenotype, deregulated metabolism and cell cycle withdrawal. Adapted from Gorgoulis et al.⁶⁷.

1.7 The Role of STAT3

An inflammatory tumor environment is known to initiate or promote tumor formation⁷⁸⁻⁸⁰. It is marked by the presence of inflammatory cells and mediators such as chemokines and cytokines. *Signal Transducer and Activator of Transcription 3 (STAT3)* is a transcription factor which contributes to an inflammatory and carcinogenic tumor environment and is upregulated in many cancer types, including melanoma⁸¹. Its persistent activity in tumors is important for the initiation, progression and maintenance of cancer through regulation of cell proliferation, survival, differentiation, immune responses, angiogenesis and stem cell maintenance⁸². STAT3 proteins have dual roles as transducers of cell signals through the cytoplasm and as nuclear transcription factors. They maintain a proinflammatory state by recruiting and activating immune cells and tumor cells through production of cytokines (e.g. IL-6, IL-1 β , IL-8, IL-21)⁸¹.

Continuous activation of STAT3 in cancers is one of the drivers in their tumor biology but it has also been shown that constitutively active *STAT3* (STAT3-C) itself acts as an oncogene and is able to mediate transformation of fibroblasts, forming tumors in mice⁸³. In melanoma however, *NRAS* specific STAT3 signaling was not yet described, especially in the context of codon-dependent mutational differences.

1.8 Aim of the Thesis

Current literature implies that *NRAS*^{Q61} and *NRAS*^{G12/13} mutations cause different phenotypic characteristics in human melanoma. To confirm this observation, we focused on the phenotypic effect of different *NRAS* mutations on both, primary human melanocytes and in melanoma-like immortalized human melanocytes. Secondly, our objective was to reveal the differential activation of cellular signaling pathways initiated by these *NRAS* mutations and to answer the question, how *NRAS* exerts its transforming capability.

Here, we identify STAT3 as a pathway upregulated in *NRAS*^{Q61} but not in *NRAS*^{G12/13} mutated melanocytic cells. STAT3 activation is associated with a more tumorigenic phenotype of primary and immortalized melanocytes and melanoma cell lines. This data gives insight into a deeper understanding of *NRAS*-associated pathways and might contribute to improve therapeutic approaches to successfully treat *NRAS*-mutated melanoma for which successful targeted therapy is still difficult.

2 MATERIAL AND METHODS

2.1 Materials

2.1.1 Reagents and Kits

Product	Company	Catalog No.
Alamar Blue®	Invitrogen	DAL1100
Ampicillin	Carl Roth	HP62.1
Ammonium Persulfate (APS)	Carl Roth	9592
BSA-Powder, Albumin Fraction V	Carl Roth	8076.2
Complete Mini Protease Inhibitor Cocktail	Roche Diagnostics	4693159001
DH5α Competent Cells	Thermo Fisher Scientific	18265017
Endofree Plasmid Maxi Kit	Qiagen	12362
High Performance Chemiluminescence Film	GE healthcare	28906836
Human Cytokine Array	R&D Systems Europe	ARY005B
Human Phospho-RTK Array Kit	R&D Systems Europe	ARY001B
Immobilon PVDF membrane, 0.45µM	Merck Millipore	IPVH00010
Luminata Forte Western HRP Substrate	Merck Millipore	WBLUF0500
MicroAmp Optical 96well Plate qPCR	Thermo Fisher Scientific	N8010560
PageRuler Plus Prestained Protein Ladder	Life Technologies	26619

Paraformaldehyde	Sigma Aldrich	P6148-1KG
Pierce BCA Protein Assay Kit	Thermo Fisher Scientific	23225
PhosSTOP	Sigma Aldrich	4906845001
Qiaprep Spin Miniprep Kit	Qiagen	27106
RevertAid First strand cDNA Synthesis Kit	Thermo Fisher Scientific	K1622
Rnase-Free Dnase Set	Qiagen	79254
RNeasy Plus Mini Kit	Qiagen	74136
Senescence β -Galactosidase Staining Kit	Cell Signaling	9860
Skim milk powder	Gerbu Biotechnik	16021000
SYBR Green PCR Master Mix	Applied Biosystems	4309155
TEMED	Carl Roth	23673
TritonX-100	Carl Roth	30514
Tween® 20	Applichem	A13890500
Venor Gem Classic Myco PCR Kit	Minerva Biolabs	11-1100
X-treme GENE® 9 DNA Transfection Reagent	Roche Diagnostics	6365787001

2.1.2 Reagents for Cell Culture

Product	Company	Catalog No.
2-Mercaptoethanol	Gibco® Life Technologies	31350010
254 Medium	Gibco® Life Technologies	M254500
dbcAMP	Sigma-Aldrich	D0627
DMSO	Carl Roth	A994.2
Dulbecco's Modified Eagle's Medium (DMEM)	Thermo Fisher Scientific	10569010
Fetal Calf Serum (FCS)	Biochrom	S0115
G 418	Roche	G418-RO
Ham's F10	Gibco® Life Technologies	11550043
Human Melanocyte Growth Supplement	Gibco® Life Technologies	S0025
3-Isobutyl-1-methylxanthine (IBMX)	Sigma-Aldrich	I5879
Sodium Orthovanadate (Na ₃ VO ₄)	Sigma-Aldrich	450243
Non-essential amino acids	Sigma-Aldrich	M7145
PBS	Sigma-Aldrich	D8537
Penicillin/Streptomycin	Sigma-Aldrich	P4333
Polybrene Infection / Transfection Reagent	Sigma Aldrich	TR-1003-G
Trypan blue solution	Sigma-Aldrich	93595
Trypsin-EDTA solution	Sigma-Aldrich	T3924

2.1.3 Human Cell Lines

Cell line	Source	Description
NHM	Isolated from foreskin	Primary melanocytes
MelSTV	CNIO Madrid	Immortalized melanocytes (Gupta et al. Nat. Gen. 2005 ⁸⁴)
MeWo	CMMM, Nice, France	<i>BRAF</i> WT/ <i>NRAS</i> WT
pmel	Department of Dermatology, Brigham and Women's Hospital, Boston, USA	Immortalized melanocytes (Garraway et al. Nature 2005) ⁸⁵

2.1.4 Antibodies

Product	Company	Catalog No.
Akt (40D4, 1:5000 in 5% Milk)	Cell Signaling	CST 2920
Anti-mouse IgG, HRP-linked	Cell Signaling	CST 7076
Anti-rabbit IgG, HRP-linked	Cell Signaling	CST 7074
Axl (C44G1, 1:1000 in 5% Milk)	Cell Signaling	CST 4566
mCherry (1C51, 1:10000 in 5% Milk)	abcam	ab125096
p44/42 MAPK (Erk1/2, 137F5, 1:4000 in 5% Milk)	Cell Signaling	CST 4695
Phospho-Akt (Ser473, 193H12, 1:2000 in 5% Milk)	Cell Signaling	CST 4058
Phospho-p44/42 MAPK (T202/Y204, E10, 1:2000 in 5% Milk)	Cell Signaling	CST 9101
α -Actinin (H-2, 1:50000 in 5% Milk)	Santa Cruz	sc17829
β -Actin (13E5, 1:10 000 in 5% BSA)	Cell Signaling	CST 5125

2.1.5 Plasmids

Plasmid	Source
Empty vector	EF1 α -mCherry
NRASWT	EF1 α -NRASWT-mCherry
NRASG12V	EF1 α -NRASG12V-mCherry
NRASG12D	EF1 α -NRASG12D-mCherry
NRASG13D	EF1 α -NRASG13D-mCherry
NRASQ61K	EF1 α -NRASQ61K-mCherry
NRASQ61L	EF1 α -NRASQ61L-mCherry
NRASQ61H	EF1 α -NRASQ61H-mCherry
shRNA non targeting Control	Dharmacon, RHS4346
shSTAT3.1 TACCTAAGGCCATGAACTT	Dharmacon, V2LHS_88502
shSTAT3.2 ATAGTTGAAATCAAAGTCA	Dharmacon, V3LHS_376016

2.1.6 siRNA

siRNA	Company	Catalog No.
AllStars Negative Control siRNA	Qiagen	1027280
siSTAT3.3	Qiagen	SI00048377
siSTAT3.4	Qiagen	SI00048384

2.1.7 Primers

Target	Forward Sequence	Reverse Sequence
18S	GAGGATGAGGTGGAACGTGT	TCTTCAGTCGCTCCAGGTCT
AXL	CCGTGGACCTACTCTGGCT	CCTTGGCGTTATGGGCTTC
BEX1	GCAGTAAACAGTCTCAGCATGG	GGCTCCCCTTTATTAGCAACTT
c-myc	CTCCTCCTCGTCGCAGTAGA	GCTGCTTAGACGCTGGATT
IL1B	TGTGAAATGCCACCTTTTGA	GGTCAAAGGTTTGGAAGCAG
IL1R	ATGAAATTGATGTTTCGTCCCTGT	ACCACGCAATAGTAATGTCCTG
IL24	GACTTTAGCCAGCAGACCCTT	GGTTGCAGTTGTGACACGAT
MITF	GCTCACAGCGTGATTTTTCC	TCTCTTTGGCCAGTGCTCTT
MMP2	TACAGGATCATTGGCTACACACC	GGTCACATCGCTCCAGACT
Rb	ATCTGCTGCCGTCAACTAGAA	GATCTCGAATCAGGCGCTTAAA
SerpinB2	CAGCACCGAAGACCAGATGG	CCTGCAAAATCGCATCAGGATAA
STAT3	ATGGAAGAATCCAACAACGGCAGC	AGGTCAATCTTGAGGCCTTGGTGA
STC1	GTGGCGGCTCAAACTCAG	GTGGAGCACCTCCGAATGG
TAGLN3	ACAAGAGCCCATACCCAAGAT	TCTCCGCAGCTTTTAGGAACT

2.1.8 Solutions and Buffers

Name	Ingredients
Blocking buffer (BSA)	5% BSA
	1x TBS

Blocking buffer (milk)	5% Skim milk powder 1x TBS
Cell freezing medium	80% FCS 20% DMSO
Crystal violet solution	0.5% Crystal violet 20% Methanol dH ₂ O
LB Medium	20g LB-Medium (Carl Roth, X964.2) 1l H ₂ O
Running buffer (pH8.3)	25mM Glycine 190mM Tris 0.1% SDS dH ₂ O
TBS 10X (pH 7.6)	150mM NaCl 50mM Tris dH ₂ O
Transfer buffer (pH 8.3)	25mM Glycine 190mM Tris 20% SDS 20% Methanol dH ₂ O
Washing buffer (TBST)	0.02% Tween® 20 1X TBS

2.2 Equipment

Product	Company
12 Well Multiwell Plates	Grenier Bio-One
2100 Bioanalyzer Instrument	Agilent
6 Well Multiwell Plates	Grenier Bio-One
AB 7500 Real-Time PCR Machine	Applied Biosystems
CELLSTAR® Cell Culture Flasks	Grenier Bio-One
ChemiDoc™ Touch Imaging System	Bio-Rad
Corning Cell Scrapers	Sigma Aldrich
Culture-inserts 2 well	Ibidi
FACSCanto II	BD Biosciences
Haemocytometry	Neubauer
Leica DM LS light microscope	Leica
MicroAmp Optical 96well Plate qPCR	Thermo Fisher Scientific
Microplates 24-well	Falcon
Microplates 96-well	Falcon
Nanodrop Spectrophotometer ND-1000	Peqlab Biotechnologie GmbH
Nikon Eclipse Ti Fluorescence Microscope	Nikon
Nunc™ Cell Culture Cryogenic Tubes	Thermo Fisher Scientific
Rotilabo®-syringe filters, 0,22 µm	Carl Roth
Rotilabo®-syringe filters, 0,45 µm	Carl Roth

Tecan Infinite F200 PRO

Tecan

Veriti™ 96-Well Thermal Cycler

Thermo Fisher Scientific

2.2.1 Software Tools

Software name	Source
7500 Software v2.0.5	Applied Biosystems
Chipster	Chipster Open source
FlowJo 7.2.2	FlowJo License
GraphPad PRISM 8	GraphPad License
iControl 1.10	TECAN
Image J	NIH
NIS-Element	Nikon
TScratch	CSELab

2.3 Methods

2.3.1 Cell Culture

Human primary melanocytes were isolated from healthy donor's neonatal biopsies in accordance with the ethical regulation (Ethics committee II, University Medical Center Mannheim, Germany). Therefore, the biopsy was washed with 70% Ethanol and PBS (+1% Pen/Strep) and digested with Dispase over night at 4°C after removing the deep dermis, adipose tissue and blood vessels. The separated epidermis was incubated with Trypsin/EDTA diluted 1:1 with PBS at 37°C for 20 minutes. After adding fetal calf serum (FCS), the cell suspension was gently mixed and filtered through a 70µm cell strainer.

Isolated melanocytes were cultured in 254 Medium (Gibco™) supplemented with Human Melanocyte Growth Supplement (Gibco™) and 20µg/ml G418 in the first passages to avoid fibroblast growth.

Immortalized Melanocytes MelSTV⁸⁴, HEK293T and melanoma cell line MeWo were cultured in DMEM Medium (High Glucose, GlutaMax, Gibco™) supplemented with 10% fetal calf serum, MEM Non-essential Amino Acid Solution (Sigma-Aldrich®), 1% β-Mercaptoethanol, 1% Penicillin (100 U/ml) and Streptomycin (100µg/ml). Immortalized melanocytes pmel (Garraway et al., 2005)⁸⁵, gift from Prof. Hans R. Widlund, Department of Dermatology, Brigham and Women's Hospital, Boston, USA, were cultured in Ham's F10 (Gibco™) supplemented with 7% FCS, 1% Penicillin (100 U/ml) and Streptomycin (100µg/ml), 0.1mM IBMX, 50ng/mL TPA, 1µM Na₃VO₄ and 1µM dbcAMP. All cells were maintained at 37 °C in a humid incubator with 5% CO₂.

2.3.2 Lentiviral Transduction

Lentivirus particles were produced using X-tremeGENE™ 9 DNA Transfection Reagent (Roche) in HEK293T cells according to the manufacturer's instructions. Therefore, after

discarding the first supernatant, the virus containing supernatant was collected three times after 12 hours each.

Cells were transduced with virus supernatant and 4µg/ml Polybren two times for each 24 hours and then cultured in the corresponding maintenance medium. Cells were then sorted for mCherry positive cells by flow cytometry.

For double transduction primary melanocytes were first transduced with *STAT3* shRNA two times for each 12 hours followed by two times transduction with *NRAS* mutants.

The plasmids used were different *NRAS* mutants and shRNA against *STAT3*.

DNA encoding for *NRAS* wildtype and each mutated in either codon 12/13 (*G12V*, *G12D*, *G13D*) or codon 61 (*Q61K*, *Q61L*, *Q61H*) was cloned into a plasmid under control of an EF1α -Promoter. The *NRAS* gene was coupled with the fluorescent reporter-protein mCherry linked with an internal ribosome entry site (IRES).

Two different shRNAs against *STAT3* and a shRNA non targeting Control were used to silence *STAT3*.

2.3.3 siRNA

siRNA transfection of cells was performed using Lipofectamine RNAiMAX Transfection Reagent (Thermo Scientific) according to the manufacturer's instructions. Therefore, cells were seeded in a 6-well-plate to reach 60-80% confluency at transfection day. The Transfection Mix was prepared for a final concentration of 25pmol siRNA per well with Lipofectamine RNAiMAX Transfection Reagent resolved in OptiMEM. The Mix was added for 48 hours. After transfection cells were seeded for functional assays.

2.3.4 Senescence Quantification

Transduced primary melanocytes were stained using Senescence β -Galactosidase Staining Kit (Cell Signaling) according to the manufacturer's instructions. The number of β -Galactosidase positive cells was quantified and related to the total number of cells by manual counting using brightfield micrographs after 0, 2, 6 and 10 days. The number of vacuolized cells was also quantified independently using brightfield micrographs.

For the detection of senescence-associated heterochromatin foci (SAHF) cells were fixed with 4% paraformaldehyde for 8 minutes. After three washes with PBS, fixed cells were permeabilized with 0.1% Triton-X100 for 10 minutes, washed and stained with DAPI (Roche, 1:2000, in TBST) for 5 minutes. Before imaging cells were washed 3 times with PBS. Furthermore, SAHF were quantified with ImageJ integrated cell counter and manual counting.

2.3.5 RNA Isolation

mRNA was isolated from cell pellets using RNeasy Mini Kit and DNase I digestion for 15 minutes to remove genomic DNA according to the manufacturer's protocol. Measurements to determine RNA concentration were done with spectrophotometry using a NanoDrop ND1000 device. The RNA was then used directly or stored at -80°C.

2.3.6 cDNA Synthesis

cDNA was synthesized using cDNA Reverse Transcription Kit (Thermo Fisher Scientific™) according to the manufacturers' guidelines.

First, 500ng mRNA was mixed with 1 μ l OligoDT Primers, 2 μ l 10mM dNTP Mix, 1 μ l RevertAid M MuL-V-enzyme (200U/ μ l), 0.5 μ l RiboLock RNase Inhibitor (40 U/ μ l), 4 μ l 5x Reaction Buffer and filled up with nuclease-free dH₂O to a total volume of 20 μ l for each sample. Samples were then mixed gently and eventually incubated 60min at 42°C,

followed by an incubation at 70°C for 5min. cDNA was directly used for quantitative real-time PCR or stored at -20°C.

2.3.7 Quantitative Real-time PCR

Quantitative real-time PCR was performed using SYBR™ Green PCR Master Mix (Applied Biosystems™) and 7500 Fast Real-Time PCR System (Applied Biosystems™).

The PCR conditions programmed were: 50°C for 2 minutes, 95°C for 10 minutes, 40 cycles of 95 °C for 15 seconds, 60°C for 1 minute and 72°C for 7 seconds. CT Values were normalized to *18S* as a housekeeping gene and relative expression of genes was quantified by calculating $\Delta\Delta CT$. Primers were designed and validated with the melting curve and efficiency analysis.

2.3.8 Protein Isolation

For protein isolation Lysis Buffer was prepared. Therefore, 100µl PhosStop (1 tablet in 1ml dH₂O), 100µl Complete Mini Protease Inhibitor Cocktail, 10µl Triton X100 and 790µl TBS buffer were mixed gently and stored on ice.

After the removal of cell medium, cells were washed with PBS. Around 70-100µl Lysis Buffer was directly added on the cells and incubated for 1 minute on ice. After incubation, cell lysates were detached from the plate using a cell scraper. The cell suspension was then transferred to a tube and cell debris was pelleted through centrifugation for 15 minutes. Lastly, the supernatant containing the protein lysate was transferred to another tube and directly used for Western Blot analysis or stored at -80°C.

2.3.9 Western Blot

Protein concentration was measured using Pierce™ BCA Protein Assay Kit (Thermo Scientific™). Briefly, the samples were diluted 1:10 with dH₂O and standards were prepared according to the manufacturer's protocol. In 96-well-plates 25 µl of protein sample was then mixed with 200µl of BCA reagent and incubated at 37°C for 30 minutes. Absorbance was measured after incubation using a Tecan Infinite 200 Pro plate reader and protein concentrations were calculated with reference to the standard curve.

20-30µg protein was loaded and separated on an SDS-PAGE Gel, then wet blotted on a 0.45 µm PVDF membrane. The membranes were blocked with either 5% skim milk or 5% BSA for at least one hour at room temperature. Then, they were incubated in primary antibodies over night at 4°C followed by an HRP-linked secondary antibody for one hour at room temperature. The protein bands were visualized using Immobilon Forte Western HRP substrate and Hyperfilm ECL, according to the manufacturer's protocol.

2.3.10 Whole Genome Microarray Analysis

Labeled RNA was hybridized to whole-genome Illumina Sentrix BeadChip® array HumanHT-12 v4 (Santa Clara, CA, USA) by DKFZ Genomics and Proteomics Core Facility. Microarray scanning was carried out using an iScan array scanner. Data extraction was carried out for all beads individually, and outliers were removed when the absolute difference to the median was greater than 2.5 times MAD (2.5 Hampel's method). All remaining bead level data points were then quantile normalized. Chipster Software was used to assess fold change and p-value of differentially expressed genes between *NRASG12/13* and *NRASQ61* expressing cells.

2.3.11 Proliferation

To measure the proliferative ability, cells were plated at a density of 500 cells in a 96-well plate. After 0 and 9 days, alamarBlue™ Cell Viability Reagent (Invitrogen) was added and after 4 hours of incubation at 37°C, fluorescence was measured with excitation wavelength at 530-560nm and emission wavelength at 590nm with the Tecan Infinite 200 Pro plate reader. The fold increase of fluorescence intensity from day 9 to day 0 was calculated and plotted.

2.3.12 Colony Formation

200 cells were each plated in a 6 well-plate. Culture medium was changed every 2 to 3 days. After 11 days cells were fixed and stained with 0.05% Crystal Violet (1% formaldehyde (37%), 1% Methanol in PBS) for 20 minutes at room temperature. Cells were gently washed twice with tap water and air-dried. The area of the plate covered by stained colonies was quantified using the ImageJ Plugin ColonyArea⁸⁶.

2.3.13 Migration

To analyze the migratory potential, 35 000 cells were plated in each well of a 2-well-culture-insert (ibidi) with MEF-Medium. After cells attached to the plate 4 hours later, the medium was replaced with FCS-free MEF-Medium and cells were incubated overnight in the cell incubator. Inserts were removed the day after, and cells were washed with PBS. 10% FCS-containing MEF-Medium with 1µg/ml Aphidicolin (Sigma) was added. Cell migration was monitored with the microscope after 0 and 8 hours. TScratch Software was used for quantitative analysis of the closing gap.

2.3.14 Proteome Profiler Array

Protocol was followed by manual instructions from R&D Systems Europe, Ltd, Human Phospho-RTK Array Kit and Human Cytokine Array. Briefly, cell lysates were diluted and incubated overnight with either array. The array was washed to remove unbound proteins followed by incubation with a cocktail of biotinylated detection antibodies and with streptavidin-HRP antibodies. Captured signal corresponded to the amount of bound phosphorylated protein.

2.3.15 Statistical Analyses

The statistical analyses of experiments were performed using the students t-test with a two-tailed distribution. Experiments were performed at least in 3 biological replicates. Differences were considered as significant with a value of $p < 0.05$ (marked with *), $p < 0.01$ (marked with **), $p < 0.001$ (marked with ***) and $p < 0.0001$ (marked with ****).

3 RESULTS

3.1 *NRAS*^{G12/13} mutants induce a stronger OIS-associated phenotype than *NRAS*^{Q61} mutants in normal human melanocytes

The first step of tumor initiation in melanomagenesis is the activation of oncogenes in primary melanocytes. Oncogenes have different effects depending on the cellular setting they arise in. In primary cells, they are not able to transform cells, but they give rise to oncogene-induced senescence (OIS). So, we first investigated the effect of *NRAS* mutations on the induction of OIS in normal human melanocytes (NHM).

We thereby selected *NRAS* domains either mutated in codon 61 (*NRAS*^{Q61K}, *NRAS*^{Q61L}, *NRAS*^{Q61H}) or codon 12/13 (*NRAS*^{G12V}, *NRAS*^{G12D}, *NRAS*^{G13D}). For lentiviral transduction of NHM we designed plasmids carrying the mutation of interest. The *NRAS* gene was cloned under the control of the EIF1α -promoter. Wildtype *NRAS* (*NRAS*^{WT}) and an empty vector (vector) served as controls. As an optical reporter of successful transduction, a gene coding for fluorescent mCherry was cloned into the lentiviral plasmid right behind the *NRAS* gene after an *IRES* gene site (Figure 4).

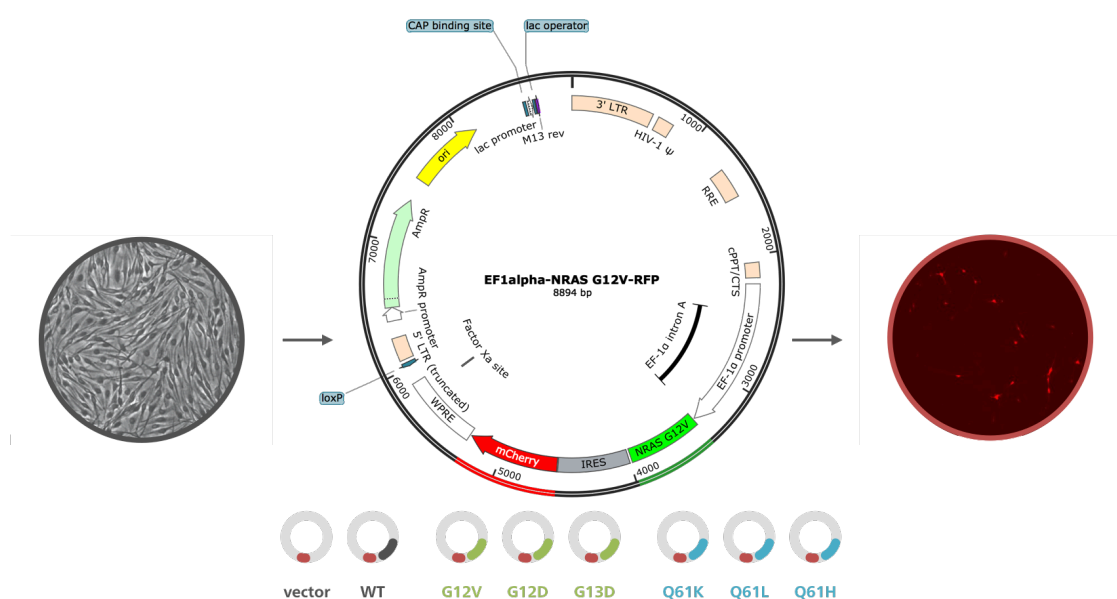


Figure 4 | Lentiviral transduction of NHM with *NRAS* mutation bearing plasmids

Schematic view of lentiviral transduction of normal human melanocytes (NHM) with plasmids carrying either an empty vector, *NRASWT*, *NRASG12V*, *NRASG12D*, *NRASG13D*, *NRASQ61K*, *NRASQ61L* or *NRASQ61H* under control of an EF1 α -Promoter. An additional *IRES* site was added for the expression of red fluorescent mCherry-protein. NHMs with successful transduction show red fluorescence.

As previously described, the expression of mutated *NRAS* in primary human melanocytes led to a senescent phenotype with higher senescence-associated- β -Galactosidase activity⁸⁷ (SA- β -Gal) and a flattened cell morphology with vacuolization of the cell body (**Figure 5A**). Control conditions of non-transduced samples (NI) or samples transduced with an empty vector or *NRASWT* showed no senescence. Moreover, the senescent phenotype was also confirmed by observation of punctuated nuclei foci, the senescence-associated-heterochromatin foci (SAHF) (**Figure 5B**). We then analyzed the number of senescent cells after transduction with the lentiviral plasmids after 0, 2, 6 and 10 days. In fact, quantification of senescent cells by SA- β -Gal-expression showed a higher percentage of senescent cells in *NRASG12V*, *NRASG12D* or *NRASG13D* mutated melanocytes with up to 69%. In contrast, melanocytes expressing *NRASQ61K*, *NRASQ61L* and *NRASQ61H*, showed only up to 46% senescent cells respectively (**Figure 5C**). The same could be observed by quantification of vacuolized cells, revealing more vacuolization in the *NRASG12/13* mutated group with up to 90% compared to *NRASQ61* with only up to 51% (**Figure 5D**).

This data confirms the different capability of *NRAS* mutations to induce senescence in primary human melanocytes indicating a higher susceptibility to OIS of NHM carrying mutations in codon 12 or 13 rather than mutations in codon 61.

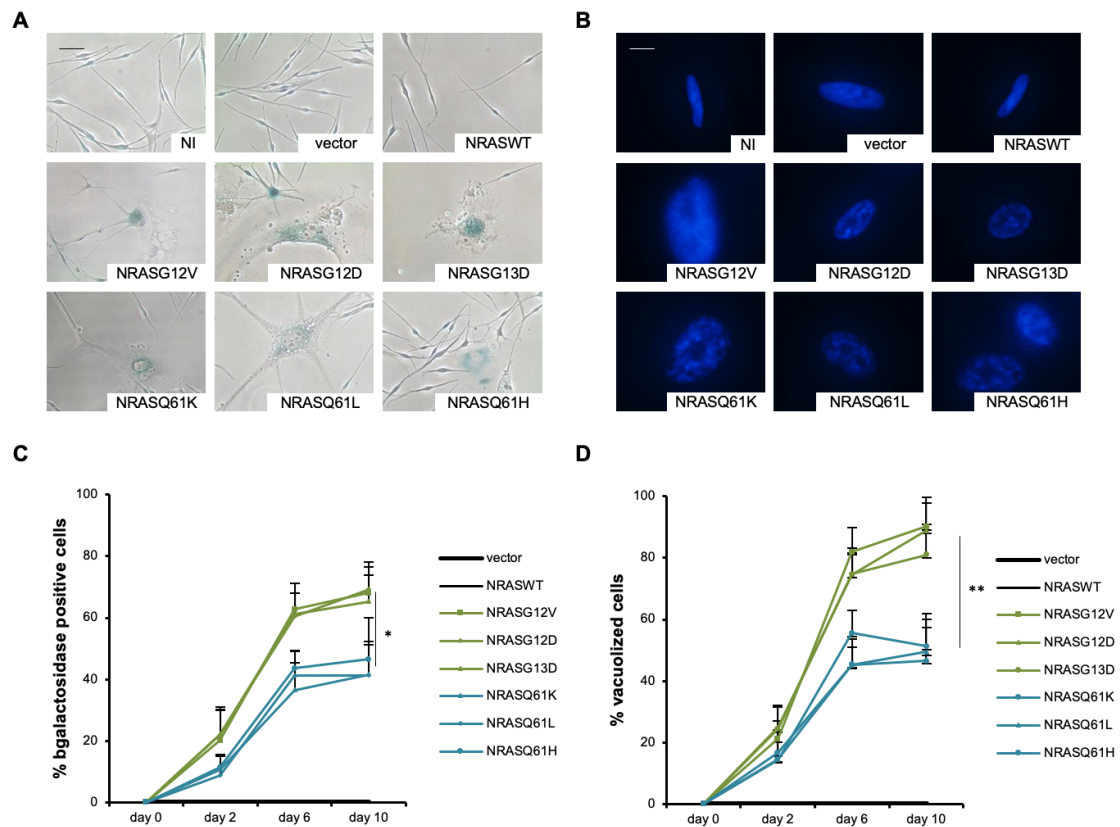


Figure 5 | *NRASG12/13* mutants induce a greater OIS-associated phenotype than *NRASQ61* mutants in NHM

A Normal human melanocytes (NHM) expressing mutated *NRAS* in either codon G12/13 or Q61 show an oncogene-induced senescence phenotype with vacuoles and a flattened morphology. Cells were stained with β-Galactosidase after 9 days. Scale bar: 100μm **B** Expression of mutated *NRAS* induces an accumulation of senescence-associated heterochromatin foci (SAHF) with enlarged punctuated nuclei. Scale bar: 20μm **C** Quantification of senescence-associated β-Galactosidase positive cells in percent after 0, 2, 6 and 10 days. **D** Quantification of vacuolized cells in percent after 0, 2, 6 and 10 days. *p<0.05 **p<0.01

3.2 *NRAS*^{Q61K} expression induces a distinct secretory phenotype, tyrosine kinase activation and gene expression compared to *NRAS*^{G12V} in NHM

That OIS can be reinforced in an autocrine and paracrine way by a senescence-associated secretory phenotype (SASP) has been already shown in melanoma (see 1.6)⁸⁸. To identify the secretome of *NRAS* mutated NHM and potential differences in the secretion of factors when comparing *NRAS*^{Q61K} and *NRAS*^{G12V} expressing NHM, we analyzed the supernatant of these cells by ELISA. In accordance with current literature, secretion of well described SASP-associated cytokines was increased in *NRAS*^{Q61K} and *NRAS*^{G12V} when compared to *NRAS*^{WT} and the empty vector (Supplementary Figure 1). Additionally, our analysis revealed a differential upregulation of a cytokine panel in *NRAS*^{Q61K} expressing cells compared to *NRAS*^{G12V} expressing cells. *NRAS*^{Q61K} mutants showed an increased secretion of CXCL11, CCL1, IL-1 β , PAI-1 and CCL3/CCL4 whereas *NRAS*^{G12V} mutants showed a shift towards IL-12 p70 and CCL2 (Figure 6A). However, IL-6 and IL-8, other known components of the SASP, were upregulated in both, *NRAS*^{Q61K} and *NRAS*^{G12V}, compared to the wildtype control and empty vector but showed no significant difference, stating a similar upregulation in both conditions.

We additionally analyzed the effect of *NRAS* mutations on the activation of different receptor tyrosine kinases. Phosphorylation status of relevant tyrosine kinases was obtained using a receptor tyrosine kinase ELISA assay. These showed a panel of kinases especially activated in *NRAS*^{Q61K} mutants compared to *NRAS*^{G12V} (Figure 6B). Among them were INSR, IGF1R, AXL, VEGFR, EphA6 and EphB3.

We also investigated the regulation of genes involved in OIS. We found a reduced expression of *Rb* in *NRAS*^{Q61K} mutants compared to controls and *NRAS*^{G12/13} (Figure 6C). Moreover, *ATM*, a relevant gene of cell DNA damage repair (DDR) mechanisms, was also significantly reduced in *NRAS*^{Q61K} expressing cells when compared to *NRAS*^{G12/13} and controls.

Microphthalmia-associated transcription factor (MITF) is a gene responsible for pigmentation and melanocyte development and is also expressed in melanoma^{85,89,90}.

High doses of *MITF* promote proliferation, differentiation and survival. However, low doses of *MITF* are associated with invasion, senescence evasion and resistance mechanism to targeted therapy^{91,92}. Furthermore, low expression of *MITF* is associated with higher expression of the tyrosine kinase AXL⁹³. This so called ‘inversely correlated low MITF/AXL ratio’ could also be found in our NHM expressing mutant *NRAS*. Mutations in the *NRAS* gene led to repression of the *MITF* gene when expressed in NHM (Figure 6D). A higher repression could be observed when *NRASQ61* was expressed compared to *NRASG12/13* – 30% vs. 15% respectively. This finding was inversely correlated with the expression of the kinase AXL in a dose-dependent manner.

As the results indicate, *NRASG12/13* and *NRASQ61* mutations are each associated with a panel of specific cytokines expression and kinases activation. Additionally, lower levels of senescence associated genes *Rb* and *ATM* and a low *MITF*/AXL ratio could be confirmed in *NRASQ61* mutants compared to *NRASG12/13*.

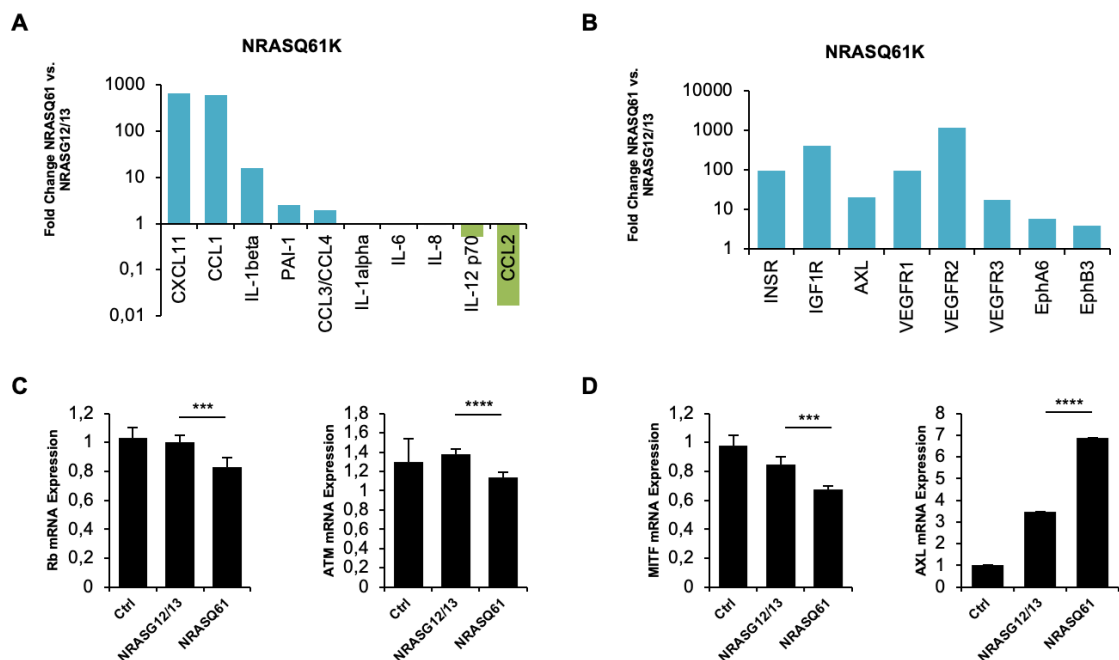


Figure 6 | *NRASQ61* expression induces a distinct secretory phenotype, tyrosine kinase activation and gene expression compared to *NRASG12V* in NHM

A Secretion of OIS-associated cytokines measured by ELISA visualized as fold change from *NRASQ61K* (blue) to *NRASG12V* (green). **B** Tyrosine kinase activity visualized as fold change from

NRAS^{Q61K} to *NRAS*^{G12V}. **C** Senescence associated mRNA expression of *Rb* and *ATM* is decreased in *NRAS*^{Q61} expressing NHM compared to *NRAS*^{G12/13} expressing cells. Values were normalized to Ctrl and shown as fold change. **D** mRNA expression of *MITF* and *AXL* is inversely correlated in *NRAS*^{G12/13} transduced cells compared with *NRAS*^{Q61} transduced cells. Values were normalized to Ctrl and shown as fold change. *** $p < 0,001$, **** $p < 0,0001$

3.3 The STAT3 Pathway is differentially activated by *NRAS*^{Q61} and *NRAS*^{G12/13} in NHM.

Activated *RAS* can affect many different downstream signaling pathways in cancer which are well described⁴⁸. To understand which underlying signaling pathways are crucially involved in the occurrence or circumvention of mutant *NRAS*-induced-senescence, we first analyzed the known deregulated pathways ERK/MAPK- and PI3K/AKT-signaling and their phosphorylation status.

Interestingly, there were no significant differences in activation of these pathways between *NRAS* mutations (**Figure 7A**). In control conditions, non-infected (nl), empty vector (vector) and *NRAS*^{WT}, ERK showed a weak basal phosphorylation. As expected, this phosphorylation increased similarly among all *NRAS* mutants whereas total ERK expression was unchanged in all conditions. No distinct activation favoring one mutant was found. The same could be observed for the PI3K/AKT-pathway. AKT phosphorylation as well as total AKT expression were not significantly changed in all conditions. We used α -Actinin, a housekeeping gene, as a loading control and equal mCherry expression allowed us to verify comparable *NRAS* transgenes expression.

To reveal other genes and pathways involved, we performed a whole genome gene expression analysis of the different *NRAS* mutants (**Supplementary Figure 2**). As expected, there was only a small group of in total 43 genes which were differentially regulated between codon 12/13 and codon 61 mutations clustering them into two groups (**Supplementary Table 1**). We found upregulated genes in the codon 61 mutation group compared to codon 12/13, such as *Transgelin3*, *BEX1*, *STC1* and

SerpinB2. Also, several *STAT3*-inducing interleukins, such as IL-24 and IL-1 β , were upregulated in the codon 61 mutation group^{94,95}. Higher mRNA expression of these genes could be confirmed by real time quantitative PCR (**Figure 7B**). The top four genes *Transgelin3*, *BEX1*, *STC1* and *SerpinB2* showed at least an increase of 100% when comparing NHM *NRAS* codon 61 mutants (61) to NHM *NRAS* codon 12 mutants (12), whereas no expression was detected in the *NRASWT* and empty vector control (Ctrl). We saw similar results in the expression levels of the interleukins *IL-24* and *IL-1 β* . An increase of these interleukins was observed in *NRASQ61* compared to *NRAS12/13*, doubling for *IL-24* and even quadrupling for *IL-1 β* .

As the screen of genes showed several genes associated with the *STAT3* pathway, we investigated the regulation of *STAT3* in the different *NRAS* mutants. The western blot analysis revealed in fact a higher phosphorylation of *STAT3*, especially in *NRASQ61* cells compared to *NRASG12/13* cells, up to 20 times higher respectively (**Figure 7C**). The controls (nl, vector and *NRASWT*) showed no activation of *STAT3*. The total expression of *STAT3* was equal along all conditions.

As we have already seen an upregulation of the *AXL* gene in NHM expressing *NRASQ61*, we confirmed the upregulation of *STAT3*-inducer tyrosine kinase *AXL* also on protein level by Western Blot analysis.

To verify the involvement of *STAT3* in the phenotypical differences of mutant *NRAS*-induced OIS, we next performed loss-of-function experiments. Therefore, we double transduced NHM with the *NRAS* mutations and subsequently with two shRNAs against *STAT3* (sh*STAT3.1* and sh*STAT3.2*) (**Figure 7D**). The silencing led to a significant decrease of *STAT3* mRNA expression in all conditions (**Figure 7E**). In fact, *STAT3* silencing efficiency reached an average of 40% mRNA reduction with both shRNAs.

We again quantified OIS by counting vacuolized cells and detected an increase of at least double of senescent cells after *STAT3* silencing in *NRASQ61* expressing NHM compared to the corresponding non-targeting shRNA control sample (shSCR) (**Figure 7F**). In contrast, no significant changes in OIS levels could be observed in *NRASG12/13*

expressing NHM after *STAT3* silencing.

Taken together, we showed that a specific activation of *STAT3* signaling by *NRASQ61* leads to lower occurrence of OIS compared to *NRASG12/13* in NHM, which can be impaired by *STAT3* silencing. These findings strongly point to a crucial involvement of *STAT3* signaling in *NRASQ61*-mediated oncogene activation.

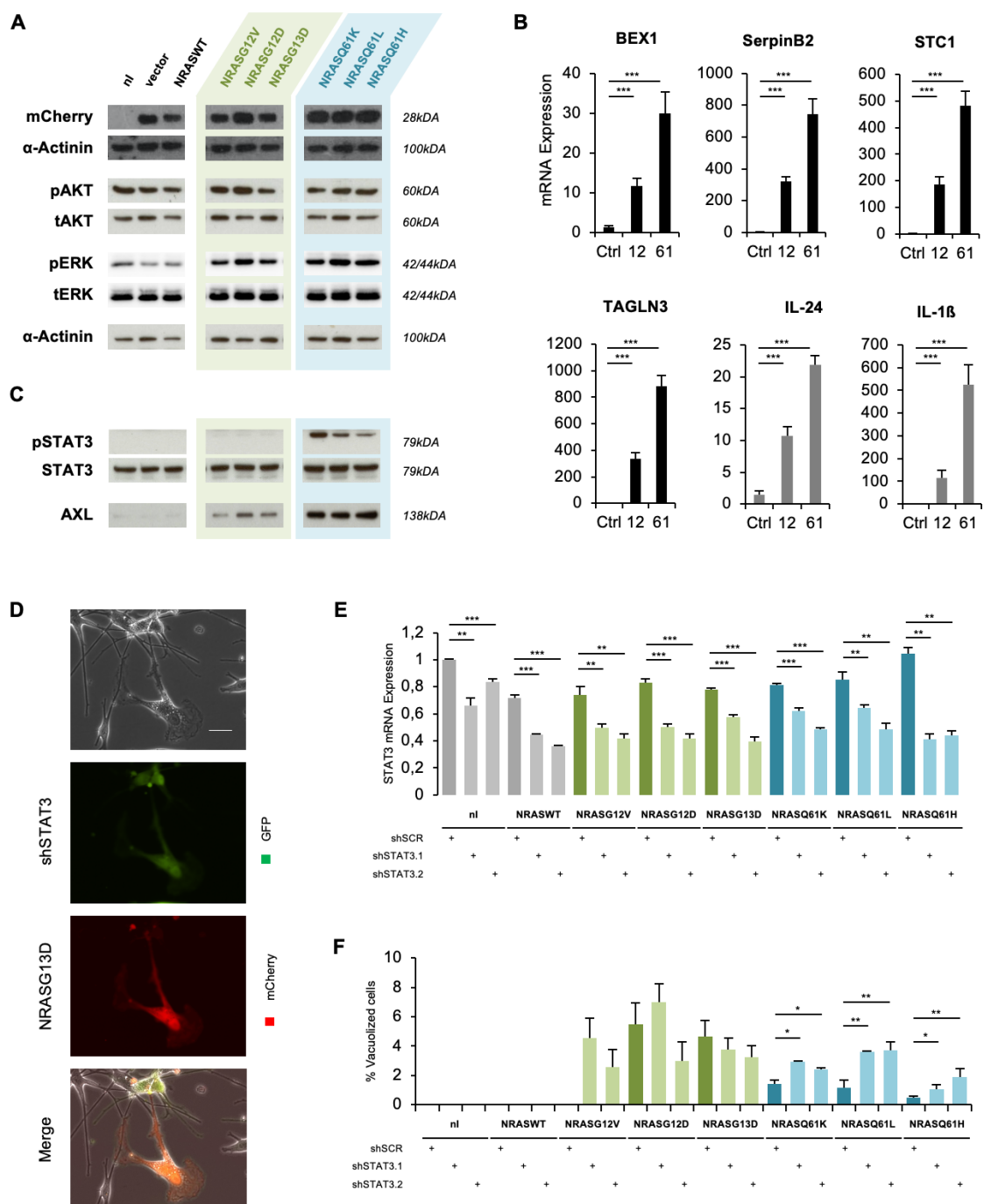


Figure 7 | The STAT3 Pathway is differentially activated by *NRAS*^{Q61} and *NRAS*^{G12/13} in NHM.

A Western Blot Analysis of mCherry expression as a reporter protein for NHM expressing no, wildtype *NRAS* or *NRAS* either mutated in codon 12/13 or codon 61 on day 4 after lentiviral transfection. Protein Analysis of phosphorylation of major signaling pathways PI3K/AKT, MAPK/ERK shows no significant differences in activation. **B** *BEX1*, *SerpinB2*, *STC1*, *TAGLN3*, *IL-24* and *IL-1 β* mRNA levels in NHM expressing either *NRAS*^{WT}, *NRAS*^{G12/13} or *NRAS*^{Q61}. Values were normalized to Ctrl and shown as fold change relative to 18S. **C** Western Blot Analysis of STAT3 activation shows higher phosphorylation status in *NRAS*^{Q61}- compared to *NRAS*^{G12/13}-expressing NHM. **D** Representative pictures of double transduced NHM expressing both *shSTAT3* (green) and mutated *NRAS*^{G13D} (red) by light and fluorescence microscopy. Scale bar: 100 μ m **E** mRNA expression levels of *STAT3* in NHM after double infection with *shSTAT3* and *NRAS* mutants. Values were normalized to nl shSCR and shown as fold change. **F** Quantification of vacuolized cells in percent. * $p < 0.05$ ** $p < 0.01$ *** $p < 0.001$

3.4 *NRAS*^{Q61H} increases proliferation, migration and colony formation of immortalized melanocytes MelSTV greater than *NRAS*^{G12V} and associates with STAT3 activation

We demonstrated that the introduction of oncogenes in primary cells alone is insufficient to form tumors due to OIS as an anti-tumor response mechanism (see 1.6). *TERT* mutations have been identified as early alterations, e.g. in intermediate skin lesions and melanoma in situ, favoring the escape from replicative senescence and survival of cells to progress to melanoma with additional mutations⁹⁶. Imitating this evolution of melanoma, we used immortalized melanocytes MelSTV to further study transforming effects of our *NRAS* mutants. These are melanocytes which were modified by Gupta et al. with a SV40ER (Simian Virus 40 early region) and hTERT (telomerase holoenzyme) region⁸⁴.

MelSTV cells have been stably transduced with *NRAS*^{WT}, *NRAS*^{G12V} or *NRAS*^{Q61H} and were each FACS-sorted to maintain a pure cell population expressing the transgene.

With this stable *NRAS* mutated cell lines we performed functional assays to monitor differences in proliferative, migratory and colony forming capacities.

First, we investigated proliferation in cell viability assays (**Figure 8A**). After nine days a significant increase of viable cells was observed in the *NRASQ61H* (72%) expressing tumor cells compared to *NRASG12V* (39%) and wildtype controls (54%), seen by measurement of increased fluorescence activity. Proliferation rates of *NRASG12V* expressing cells were slightly, but not significantly decreased compared to *NRASWT*.

Additionally, we compared the ability of MelSTV harboring the *NRAS* mutations to survive and form colonies on a single cell level (**Figure 8B**). Colony formation assays showed a higher colony forming capacity for *NRASQ61H* mutants with more than twice as much colonies covering the plate when compared to *NRASG12V* or *NRASWT* mutants. *NRASG12V* showed a tendency to form more colonies than *NRASWT*, although it was not statistically significant.

Besides local growth of a tumor cell, metastatic spread is an important hallmark in cancer⁹⁷. To examine metastatic ability of the different *NRAS* mutants, scratch-like experiments were performed (**Figure 8C**). Migration, measured by gap closure after 8 hours, was not altered when comparing *NRASWT* and *NRASG12V* expressing MelSTV. However, *NRASQ61H* was able to accelerate gap closure notably almost twice as much, suggesting a higher migration rate of *NRASQ61H* transduced cells (64% vs. 33%).

These results indicate that *NRASQ61H* induces a much more aggressive phenotype compared to *NRASG12V* when expressed in immortalized melanocytes which is consistent with our previous findings in normal human melanocytes.

To evaluate the role of STAT3 in *NRASQ61H* signaling, the phosphorylation status of STAT3 was determined in MelSTV. In line with the findings in normal human melanocytes, STAT3 was highly activated in *NRASQ61H* mutants compared to *NRASG12V* mutants and wildtype controls (**Supplementary Figure 3**).

To proof STAT3 as the mediator of the *NRASQ61H*-induced oncogenic phenotype of

affected cells, functional assays were repeated after silencing experiments with small interfering RNA against *STAT3* (siSTAT3.1 and siSTAT3.2) or a control siRNA (siSCR). After 48 hours *STAT3* levels were significantly reduced on protein and mRNA level (**Figure 8D**). The silencing efficiency at the mRNA level reached around 90% with both siRNAs in all three *NRAS* conditions. Accordingly, *STAT3* silencing with either siRNA led to a strong reduction of the total *STAT3* protein expression and reduced the amount of phosphorylated *STAT3* (62% and 42%) (**Figure 8E**). However, *STAT3* silencing significantly reduced *STAT3* phosphorylation to a similar basal level in all three *NRAS* conditions.

Reduced activation of *STAT3* impaired the formation of colonies in MelSTV in a *STAT3* dose dependent manner in all conditions (**Figure 8F**). In *NRAS* mutants transfected with siSTAT3, less colonies could be noted when compared to non-silenced controls, more in siSTAT3.1 than in siSTAT3.2 showing a dosage dependency on *STAT3* expression in all *NRAS* mutants. Additionally, gap closure in migration assays was slowed down when transiently knocking down *STAT3* (**Figure 8G**). However, both colony formation and migration were reduced in a similar manner between *NRASQ61H* and *NRASG12V* phenotypes.

Taken together, our data supports findings that *NRASQ61H* increases proliferation, migration and colony formation of immortalized melanocytes MelSTV greater than *NRASG12V*. Additionally, we identify *STAT3* as a key actor of *NRAS*-driven migration and colony formation in MelSTV, independent of their *NRAS* mutational status.

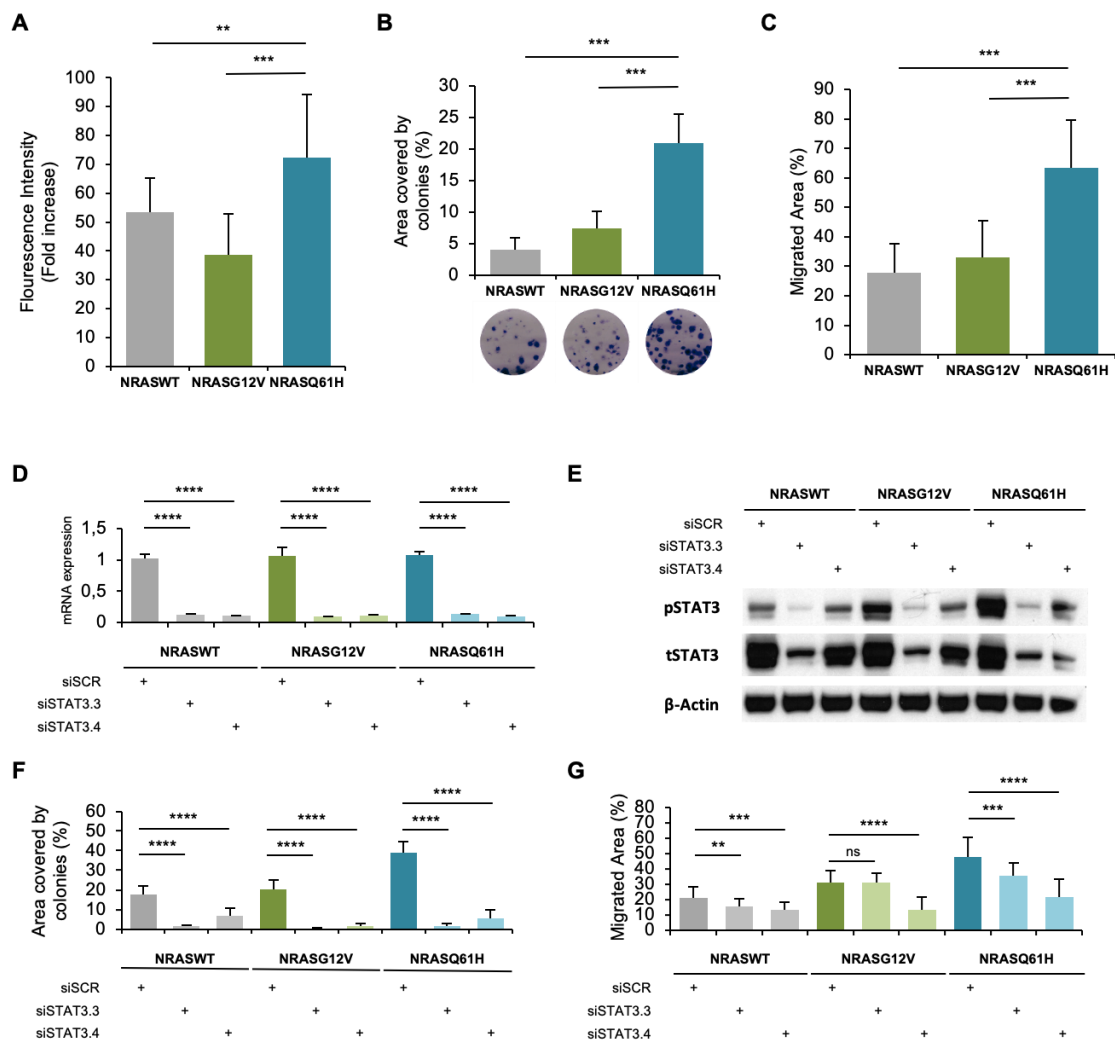


Figure 8 | *NRAS^{Q61H}* increases proliferation, migration and colony formation of immortalized melanocytes MelSTV greater than *NRAS^{G12V}* and associates with STAT3 activation

A Proliferation of MelSTV is increased when expressing *NRAS^{Q61H}* more than *NRAS^{G12V}* and *NRAS^{WT}*. Proliferation rate was measured by fluorescence intensity using Alamar Blue Assay after 9 days. **B** Colony formation is increased after 11 days when expressing *NRAS^{Q61H}* more than *NRAS^{G12V}* and *NRAS^{WT}*. **C** After 8 hours MelSTV expressing *NRAS^{Q61H}* migrate faster than *NRAS^{G12V}* and *NRAS^{WT}*. **D** mRNA expression of *STAT3* after siSTAT3 transfection after 48 hours. Values were normalized to *NRAS^{WT}* siSCR and shown as fold change. **E** Westernblot analysis of phospho-STAT3 and STAT3 levels after siSTAT3 transfection after 48 hours. **F** Colony formation of MelSTV is decreased after siSTAT3 transfection. **G** Migration of MelSTV is decreased after siSTAT3 transfection. * $p < 0.05$ ** $p < 0.01$ *** $p < 0.001$ **** $p < 0.0001$

3.5 Upregulation of *MMP2*, *IL-1 β* and *IL1R* is STAT3 mediated

Based on these findings we focused on studying STAT3 target genes which mediate the phenotypic differences between *NRASQ61H* and *NRASG12V* in MelSTV.

Both target genes *MMP2* and *c-myc* were upregulated only in *NRASQ61H* expressing cells compared to *NRASG12V* and *NRASWT*, concordant with STAT3 activation (**Figure 9A**). Also, STAT3 regulated interleukin *IL-1 β* was upregulated in *NRASQ61H* compared to *NRASG12V* and *NRASWT*⁸¹ (**Figure 9B**). In *NRASG12V* mutants *IL-1 β* expression was even decreased when compared to *NRASWT* which, however, was not statistically significant.

STAT3 silencing was able to reverse the upregulation of *MMP2*, *IL1R* and *IL-1 β* in all conditions (**Figure 9C-E**).

In contrary, the analysis of *c-myc*, another target gene of STAT3, showed an increase of its expression after STAT3 silencing (**Supplementary Figure 4**).

In summary, this data implies that the aggressive phenotype of *NRASQ61H* mediated melanomagenesis is regulated by STAT3 and its target genes *MMP2*, *IL-1 β* and *IL1R*.

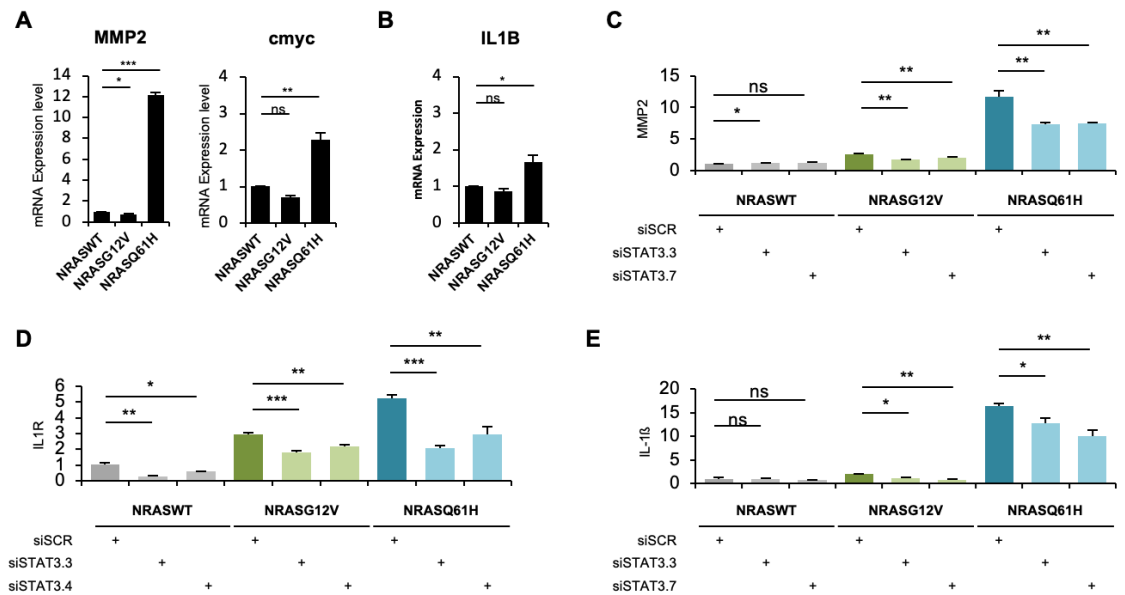


Figure 9 | Upregulation of *MMP2*, *IL-1 β* and *IL1R* is STAT3 mediated

A mRNA expression levels of *STAT3* target genes *MMP2* and *c-myc* correlate with the functional activity of *NRASQ61H* expressing MelSTV. Data was normalized to *NRASWT* and shown as fold change. **B** mRNA expression of *IL-1 β* is increased in *NRASQ61H* expressing cells compared to *NRASG12V* and *NRASWT*. Data was normalized to *NRASWT* and shown as fold change. **C** mRNA expression of *MMP2* is decreased after siSTAT3 transfection after 48 hours. Data was normalized to *NRASWT* siSCR and shown as fold change. **D** mRNA expression of *IL1R* is decreased after siSTAT3 transfection after 48 hours. Data was normalized to *NRASWT* siSCR and shown as fold change. **E** mRNA expression of *IL1B* is decreased after siSTAT3 transfection after 48 hours. Data was normalized to *NRASWT* siSCR and shown as fold change. ns=not significant * $p<0.1$ ** $p<0.01$ *** $p<0.001$

3.6 *NRAS*^{Q61H} shows increased tumorigenesis in melanoma cell lines

We could confirm these findings of more tumorigenic *NRAS*^{Q61H} over *NRAS*^{G12V} in a melanoma cell line MeWo and in immortalized melanocytes pmel.

Colony formation was higher with *NRAS*^{Q61H} than with *NRAS*^{G12V} or *NRAS*^{WT} in these two cell lines which was correlated with an increased STAT3 phosphorylation as observed by western blot (Figure 10A-B).

These results indicate that *NRAS*^{Q61H} induces a stronger tumorigenic phenotype in immortalized melanocytes and melanoma cell lines when compared with *NRAS*^{G12V}. This effect correlates with an increased STAT3 phosphorylation status.

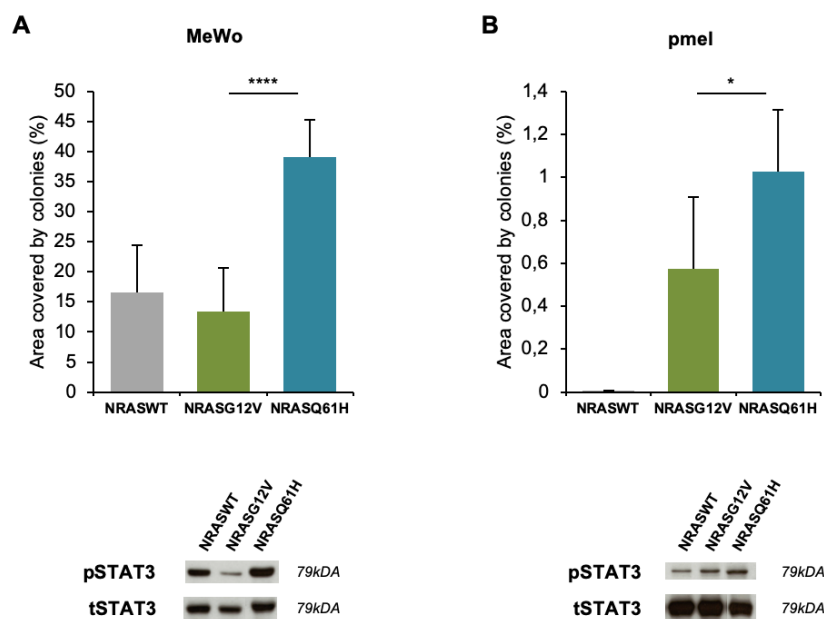


Figure 10 | *NRAS*^{Q61H} shows increased tumorigenesis in melanoma cell lines

A Expression of *NRAS*^{Q61H} in wildtype *NRAS* melanoma cell line MeWo increases ability to form colonies more than *NRAS*^{G12V} and *NRAS*^{WT} and correlates with higher STAT3 activation confirmed by Western Blot. **B** Expression of *NRAS*^{Q61H} in immortalized melanocytes pmel increases ability to form colonies more than *NRAS*^{G12V} and *NRAS*^{WT} and correlates with higher STAT3 activation. n>3 * p<0,05, ** p<0,005, **** p<0,0001.

4 DISCUSSION

4.1 *NRAS*^{Q61} shows a more tumorigenic phenotype than *NRAS*^{G12/13}

In this study, we have demonstrated a more aggressive phenotype of *NRAS*^{Q61} mutations when compared to *NRAS*^{G12/13} in the melanocytic lineage. To our knowledge, there are only few studies investigating differences between *NRAS* mutants in melanoma. Other studies have already pointed at relevant differences, not only between *RAS* isoforms *NRAS*, *KRAS* and *HRAS*, but also in codon mutational status with important clinical implications, e.g. different therapy responses to Cetuximab therapy in colorectal cancer or prognostic relevance in non-small-cell lung cancer (see 1.5.3)^{56,98,99}.

Concordant studies conclude that *RAS* mutations are seen as early events occurring in premalignant lesions in the skin and are able to initiate cancer⁵³. Therefore, we first compared the effect of *NRAS* mutants on oncogene-induced senescence in primary melanocytes to determine early effects. We found that *NRAS*^{Q61} mutant melanocytes show less oncogene-induced senescence than melanocytes expressing *NRAS*^{G12/13} (Figure 5C, D). To our knowledge, there has been no studies up to date which compare the induction of oncogene-induced senescence through different *NRAS* codon mutants in primary human melanocytes. Not only has *NRAS* expression in melanoma different properties regarding its codon mutational status, but it also affects natural cell mechanisms to prevent cancer initiation. Melanoma, which derives from a nevus, is harboring mutations in *BRAF* and *NRAS*. Especially noteworthy is that benign lesions are more likely to have *BRAF* mutations, whereas intermediate lesions carry *NRAS* mutations in the first place^{4,96}. In contrast to a high mutation burden of *BRAF* in common acquired nevi, *NRAS* mutations are found most frequently in congenital nevi (80%)¹⁰⁰. When characterizing the *NRAS* mutations in detail, there are mutations exclusively in codon 61. The absence of lesions carrying codon 12/13 *NRAS* mutations may support our findings that *NRAS*^{Q61} is able to bypass senescence and form malignant tumors with additional transforming events, but not *NRAS*^{G12/13}. In contrast, another study comparing the

mutational status of melanoma and their precursor nevi concludes that there is no significant difference in the frequency of *NRAS* mutations between nevi and melanoma, emphasizing the fact that *NRAS* mutational status itself is not a prognostic factor for melanoma formation¹⁰¹. However, more investigation is needed to understand the selection of *NRASQ61* mutants in benign primary lesions and their transformative development to malignant melanoma.

Around 30% of melanomas arise from preexisting nevi¹⁰². These melanomas share a concordant mutational status with their associated nevi, supporting the theory of a melanoma progressing within a nevus through transforming events^{103,104}. After an initial oncogenic gene alteration, further transforming events are needed to develop malignant melanoma. These are mostly secondary or tertiary genetic alterations affecting *TERT* or *CDKN2A*^{96,105}.

To investigate further effects of the different *NRAS* codon mutants, we therefore used immortalized melanocytes modified in the TERT promoter⁸⁴. When expressed in MelSTV, we found that *NRASQ61H* increases proliferation, migration and colony formation compared to *NRASG12V* (**Figure 8A-C**). These observations confirm *NRASQ61H*'s nature to be more oncogenic and are in line with data that showed higher nevus and melanoma formation in *NRASQ61R* than in *NRASG12D* expressing p16^{INK4a}-deficient mice⁵⁸.

Taken together, our data from normal human melanocytes and immortalized melanocytes shows clearly that *NRASQ61* is not only bypassing oncogene-induced senescence, but also transforms already proliferating melanocytes to tumor cells with higher tumorigenic capacities than *NRASG12/13*.

4.2 STAT3 as a driver in *NRAS*-mediated melanomagenesis

As our results showed distinct phenotypical differences between *NRAS* mutations, we analyzed the underlying molecular mechanisms and identified STAT3 as a driver, especially in *NRASQ61*-mediated melanomagenesis. Therefore, we give insight into cells

differential activation of pathways in *NRAS* mutant melanoma explaining different oncogenic potential and tumor behavior between *NRAS* mutants in the melanocytic lineage.

Analysis of commonly deregulated downstream signaling pathways PI3K-AKT and MEK-ERK showed equal phosphorylation levels (**Figure 7A**). Thus, activity variations of *RAS* might not be sufficient to explain such phenotypical differences seen in melanocytes and suggest a mutation-specific activation of additional pathways downstream of *NRAS*. Consistent with our results, the phosphorylation status of ERK and AKT showed variant expression levels in a transgenic mouse melanoma model with either *NRASQ61R* or *NRASG12D* mutational status without clear correlation⁵⁸. On the basis of a biochemical analysis, a higher activation of the *NRASQ61R* protein compared to *NRASG12D* could be found with differences in nucleotide binding, hydrolysis and stability. Similar phosphorylation levels of known downstream signaling pathways ERK and AKT may argue that this mechanism is the only explanation for the phenotypical differences *NRAS* codon mutations present.

However, in a phosphoproteomic approach Posch et al. detected higher activation of MAPK-signaling in *NRASQ61L* expressing melanocytes, whereas the *NRASG12V*-expressing counterparts showed higher PI3K/AKT-signaling¹⁰⁶. These conflicting data may be explained by different transduction kinetics.

With regard to another study focusing on PREX2, a guanine-nucleotide exchange factor, other factors modulating *RAS* activity may contribute to the differential effect on the phenotype. In their study, *PREX2* mutations in the context of *NRAS* mutational status were shown to enhance the proliferation rate of melanoma cells through activation of GEF Rac1¹⁰⁷.

Epigenetic changes were shown to cooperate with *NRAS* mutations in order to contribute to myeloid transformation in hematopoietic cells¹⁰⁸. Whether epigenetic changes are initiated or favored by *NRAS* mutations in melanoma needs further

investigation, as an older study showed at least no correlation between *NRAS* or *BRAF* mutations and the occurrence of DNA-methylation¹⁰⁹.

Our data reveals that *NRASQ61* exerts its higher transforming potential through STAT3 activation, both in normal human melanocytes and in immortalized melanocytes. This functional phenotype can be reversed when *STAT3* is silenced.

In fact, in colon cancer it has already been shown that mutant *NRASG12D* can suppress stress-induced apoptosis with more oncogenic potential through specific activation of STAT3¹¹⁰. This data supports our findings as *NRAS* mutations both activate STAT3, *NRASQ61* more than *NRASG12/13*.

In which ways STAT3 exerts its higher tumorigenic potential will be discussed in the following sections in normal human melanocytes and in immortalized melanocytes.

4.2.1 STAT3 in normal human melanocytes

In normal human melanocytes, we showed that *NRASQ61* is able to override senescence through activation of STAT3 whereas *NRASG12/13* lacks STAT3 activation and is more susceptible to OIS.

In skin carcinogenesis, continuous STAT3 activation in keratinocytes is correlated with enhanced proliferation, attenuated senescence and high frequency spontaneous immortalization¹¹¹. Broadly speaking, STAT3 plays a crucial role for the initiation, progression and maintenance of cancer throughout different malignancies (**see 1.7**).

With higher STAT3 activation through *NRASQ61*, a downregulation of senescence-associated genes *Rb* and *ATM* was observed (**Figure 6C**) which verifies the deregulation of OIS-pathways. Also, a low MITF/AXL ratio could be detected in these cells (**Figure 6D**) confirming a more invasive and less senescent phenotype^{91,92}.

We could further identify the secretome of *NRAS* mutated senescent cells and found differences in the secreted factors between *NRASQ61K* and *NRASG12V* (**Figure 6A**).

Furthermore, we could find a specific subset of receptor tyrosine kinases activated specifically under *NRASQ61K* expression (**Figure 6B**).

A link to effects of SASP from senescent melanoma cells to STAT3 activation was shown by previous studies that depicted a tumor promoting phenotype through the activation of STAT3 upon melanoma treatment with the secretome of senescent cells *in vitro*⁸⁸. *AXL* and *IL-1 β* were among upregulated genes, which is in line with our findings. In this manner, increased production of cytokines could account for the observed lower *NRASQ61*-induced OIS level when compared to *NRASG12/13* via a paracrine and autocrine mechanism *in vitro*.

Another STAT3 activating mechanism may be mediated through upstream kinase activities. Phosphoproteomic approaches of melanoma found a higher intensity of RTKs activation in *NRAS* mutant melanoma compared to *BRAF* mutant melanoma¹¹². They found *AXL*, *EGFR*, a spectrum of ephrins and c-MET activated. Yet, they did not compare the differential activation among *NRAS* mutants themselves. They only had two out of six codon 13 *NRAS* mutations which might favor the activation of *NRASQ61* in their analysis. Another study demonstrated an upregulated protein kinase CK2 α in *NRASQ61L* compared to *NRASG12V*¹⁰⁶. Other studies linked phosphorylation of STAT3 to the activation of CK2 α as an upstream event in human glioma cells¹¹³. Specifically, the kinases *AXL*, *IGF1R* and *VEGFR* are known STAT3 activators^{114,115}. We found STAT3 activated and a concordant *AXL* upregulation, suggesting the *AXL/STAT3* axis as a potential regulator of OIS-bypass in *NRASQ61*-induced oncogene activation. However, further studies are needed to fully understand the detailed activation mechanisms and to understand which kinase especially activates STAT3.

We demonstrated the differential upregulation of several genes *Bex1*, *SerpinB2*, *STC1* and *TAGLN3*. The role of these genes needs to be further evaluated in *NRASQ61*-induced melanoma transformation.

However, putting our results in context with the current literature, *NRASQ61* in particular seems to activate STAT3 through kinases activation, secretion of a subset of cytokines and expression of specific genes (Figure 11).

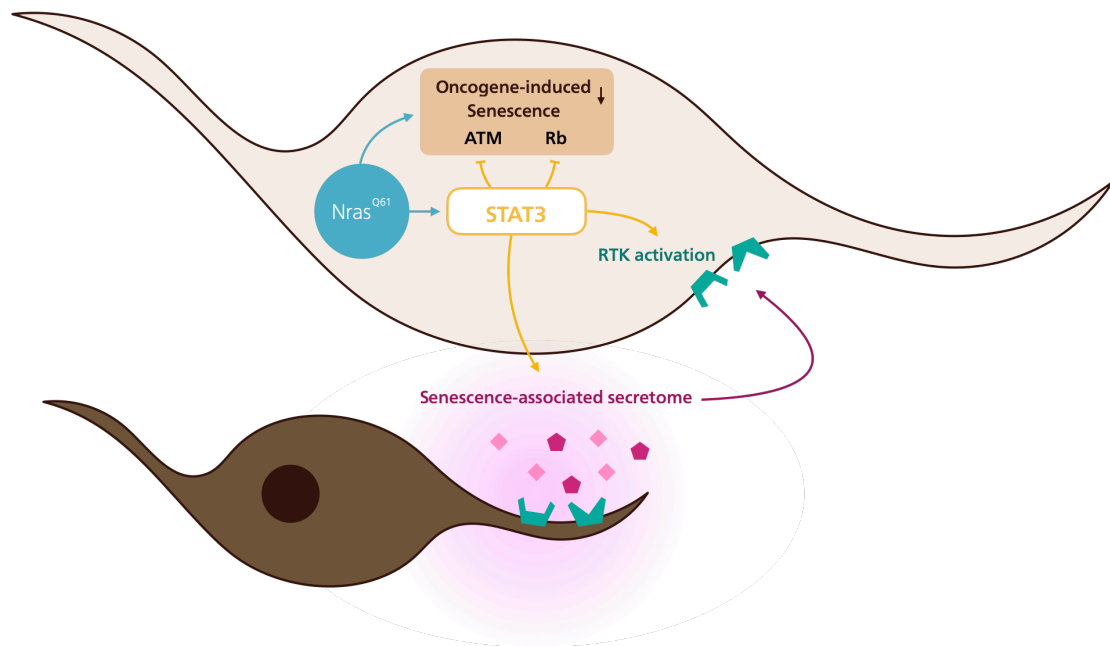


Figure 11 | NRASQ61-induced transformation

Mutations in the *NRAS* gene at locus 61 induce oncogene-induced senescence. Specific pathways, especially STAT3, are activated upon *NRASQ61* expression and leads to circumvention of senescence through downregulation of relevant genes like *ATM* and *Rb*. Further, a specific set of cytokines is secreted, the senescence-associated secretory phenotype (SASP), which itself activates autocrine and paracrine effects to promote a tumorigenic environment. Receptor tyrosine kinases (RTKs) are activated and mediate tumor transformation.

4.2.2 STAT3 in immortalized melanocytes

STAT3's activation through the mutant *NRAS* gene has been confirmed in our experiments with immortalized melanocytes MelSTV, pmel and melanoma cell line MeWo.

Downstream effectors of STAT3 were analyzed. Here we could show a STAT3 mediated upregulation of *MMP2*, *IL-1 β* and *IL1R1* in *NRASQ61* mutant MelSTV (**Figure 12**).

Melanoma with continuous STAT3 activation is shown to have an increased development of brain metastasis through upregulation of *matrix-metalloproteinase 2* (*MMP2*) which is known to be important for invasion and metastasis of melanoma¹¹⁶. Regarding clinical implications, high *MMP2* expression was shown to be an independent prognostic factor with tumor progression and worse survival rates in primary and metastatic melanoma¹¹⁷. A more migratory phenotype associated with higher STAT3 mediated *MMP2* expression could be observed in our findings as well, underlining potential invasive capabilities of *NRASQ61H* expressing cells.

Interleukin-1 β (IL-1 β) is a cytokine with pleiotropic effects on angiogenesis, inflammation, tissue remodeling immune responses which we found upregulated in *NRASQ61H* expressing MelSTV. IL-1 β is especially secreted continuously in late stage melanoma and promotes tumor development and progression^{118,119}. Analogue increase of STAT3 regulated *IL1R1* in *NRASQ61* expressing MelSTV may suggest IL1R signaling as another player in *NRASQ61* tumor transformation.

The role of *c-myc*, another target gene of STAT3, remains elusive. It is upregulated in *NRASQ61* expressing MelSTV in concordance with STAT3 activation, but even increases when STAT3 is silenced (**Supplementary Figure 4**). STAT3 is described as an upstream regulator of *c-myc*¹²⁰. Besides STAT3, small RhoGTPases (through PDGF and Src) and gamma-Catenin (WNT-signaling) are activators of *c-myc*^{121,122}. In *BRAFV600E*- as well as in *NRASQ61R*-induced senescence melanoma cell lines *c-myc* overexpression overcomes senescence, while *c-myc* depletion induces senescence in *BRAFV600E* and *NRASQ61R*

melanoma cells¹²³. *C-myc* has oncogenic properties as it regulates cell differentiation and proliferation, but also induces apoptosis^{124,125}. As *c-myc* is part of several pathways, it might not only be difficult to reduce its role to STAT3-mediated tumor transformation but may be also regulated differentially when STAT3 is silenced and is dependent on the state of tumor progression.

However, although gene silencing reduced both, *STAT3* expression and phosphorylation, the reduced tumorigenic effect on its phenotype in MelSTV did not differ in *NRASG12V* and *NRASQ61H* mutant conditions. This indicates specific STAT3 phosphorylation (Tyr705) as an important determinant for these cells tumorigenicity but may be not the only factor for *NRASQ61*-mediated tumor transformation.

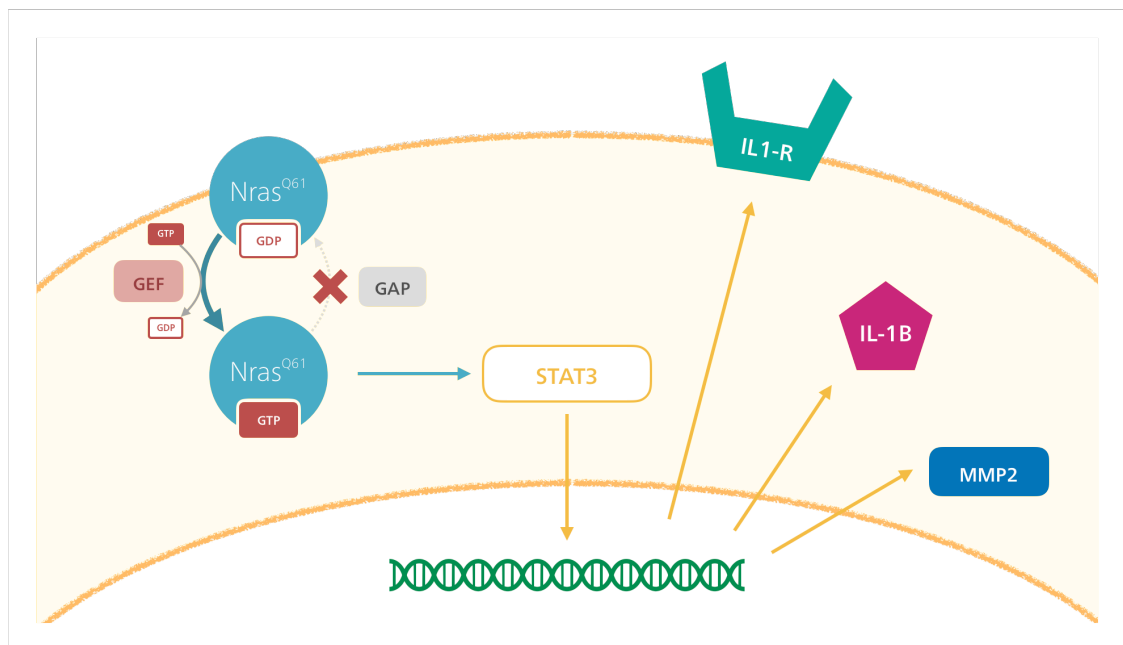


Figure 12 | *NRASQ61* activates the STAT3 pathway

NRASQ61 mutations in the melanocytic lineage activates the STAT3 pathway and leads to transcription of protumorigenic genes such as *MMP2*, *IL1-R* and *IL1-B*.

4.2.3 STAT3 inhibition as a new therapeutic option in NRAS mutant melanoma

Based on our study, for *NRAS*Q61 mutated melanoma, in particular, the combination of MEKi with inhibitors of STAT3 may be a promising therapy approach. There are already upstream kinase inhibitors which are shown to disrupt STAT3 signaling. But the low specificity and off-target effects may be limiting regarding clinical use and adverse effects¹²⁶. A new approach is to directly target STAT3. There are several preclinical compounds targeting STAT3 which show antitumorigenic effects *in vitro* and *in vivo*¹²⁶. Due to the lack of potency and its adverse effects, clinical use of STAT3 inhibitors is still limited¹²⁷. Next generation sequencing improved screening a big library of antisense oligonucleotides (ASO) for target genes. AZD9150, an ASO specifically targeting STAT3, showed promising preclinical antitumor effects *in vitro* and *in vivo*. This antitumor effect could be translated in a phase I dose-escalation study in patients with highly treatment-refractory lymphoma and non-small cell lung cancer with tolerable adverse effects and efficient anti-STAT3 activity and reduction of tumor size¹²⁸. There are several clinical phase II studies following in different solid tumors like NHL (PRISM study, NCT03527147), NSCLC, pancreatic and colorectal cancer (NCT02983578, NCT03421353). Further development of these therapeutic molecules might be a future hope for clinical use also in *NRAS* mutated melanoma.

5 CONCLUSION

In summary, we showed the different phenotypical effects of *NRASG12/13* and *NRASQ61* in the melanocytic lineage from primary to melanoma cells. In primary melanocytes *NRASG12/13* is more potent to induce oncogene-induced senescence, whereas *NRASQ61* circumvents senescence mechanisms through secretion of a set of specific cytokines and kinases activation. In immortalized melanocytes and melanoma cell lines, *NRASQ61* shows a more tumorigenic phenotype with increased proliferation, colony formation and migration. Our study gives novel insights into molecular and cellular mechanisms that are activated in response to oncogenic activation of *NRASQ61* compared to *NRASG12/13*. We therefore contribute to deeper knowledge of differences in the molecular signaling pathways of *NRAS* codon mutations. Furthermore, we give answers to the question how *NRASQ61* activates a different signaling cascade from *NRASG12/13* through activation of STAT3, as a critical mediator to initiate more oncogenic properties.

6 REFERENCES

1. Bray, F. *et al.* Global cancer statistics 2018: GLOBOCAN estimates of incidence and mortality worldwide for 36 cancers in 185 countries. *CA. Cancer J. Clin.* **68**, 394–424 (2018).
2. Howlander, N. *et al.* SEER Cancer Statistics Review, 1975-2016. *Natl. Cancer Inst.* (2016).
3. Mort, R. L. *et al.* The melanocyte lineage in development and disease. *Dev.* **142**, 620–632 (2015).
4. Bastian, B. C. *The Molecular Pathology of Melanoma: An Integrated Taxonomy of Melanocytic Neoplasia. Annual Review of Pathology: Mechanisms of Disease* vol. 9 (2014).
5. Miller, A. J. & Mihm, M. C. Melanoma. *N. Engl. J. Med.* 51–65 (2006) doi:10.1056/NEJMra052166.
6. Goldstein, A. M. & Tucker, M. A. Genetic epidemiology of familial melanoma. *Dermatologic Clinics* (1995) doi:10.1016/s0733-8635(18)30066-4.
7. Goldstein, A. M. *et al.* Features associated with germline CDKN2A mutations: A GenoMEL study of melanoma-prone families from three continents. *J. Med. Genet.* **44**, 99–106 (2007).
8. Platz, A., Ringborg, U. & Hansson, J. Hereditary cutaneous melanoma. *Semin. Cancer Biol.* **10**, 319–326 (2000).
9. Schwarz, T. 25 Years of UV-induced immunosuppression mediated by T Cells - From disregarded T suppressor cells to highly respected regulatory T cells. *Photochem. Photobiol.* **84**, 10–18 (2008).
10. Murphy, G. M. Ultraviolet radiation and immunosuppression. *Br. J. Dermatol.* **161**, 90–95 (2009).
11. Marghoob, A. A. & Alfred, W. Ultraviolet A and melanoma: A review. 837–846 (2001) doi:10.1067/mjd.2001.114594.
12. Kronforst, M. R. *et al.* DNA repair and cell cycle checkpoint defects as drivers and therapeutic targets in melanoma. *Melanoma Res.* **25**, 213–8 (2011).

13. Habits, S., Holman, D. A. J. & Armstrong, K. Relationship of Cutaneous Malignant Melanoma to Individual Sunlight-Exposure Habits. *JNCI J. Natl. Cancer Inst.* **76**, 403–414 (1986).
14. Gandini, S. *et al.* Meta-analysis of risk factors for cutaneous melanoma: II. Sun exposure. *Eur. J. Cancer* **41**, 45–60 (2005).
15. Dimitriou, F. *et al.* The World of Melanoma: Epidemiologic, Genetic, and Anatomic Differences of Melanoma Across the Globe. *Curr. Oncol. Rep.* **20**, (2018).
16. Marrett, L. D., King, W. D., Walter, S. D. & From, L. Use of host factors to identify people at high risk for cutaneous malignant melanoma. *CMAJ* **147**, 445–453 (1992).
17. Gilchrest, B. A., Eller, M. S., Geller, A. C., Yaar, R. N. & Yaar, M. The pathogenesis of melanoma induced by ultraviolet radiation. *N. Engl. J. Med.* **340**, 1341–1348 (1999).
18. Deutsche Krebsgesellschaft, Deutsche Krebshilfe & AWMF. S3-Leitlinie zur Diagnostik, Therapie und Nachsorge des Melanoms, Langversion 3.1. *Leitlinienprogr. Onkol. Version 2.*, AWMF Registernummer: 032/024OL (2018).
19. Breslow, A. Thickness, cross-sectional areas and depth of invasion in the prognosis of cutaneous melanoma. *Ann. Surg.* **172**, 902–908 (1970).
20. Garbe, C. *et al.* Diagnosis and treatment of melanoma. European consensus-based interdisciplinary guideline - Update 2016. *Eur. J. Cancer* **63**, 201–217 (2016).
21. Boespflug, A., Caramel, J., Dalle, S. & Thomas, L. Treatment of NRAS -mutated advanced or metastatic melanoma: Rationale, current trials and evidence to date. *Ther. Adv. Med. Oncol.* **9**, 481–492 (2017).
22. Mandalà, M., Merelli, B. & Massi, D. Nras in melanoma: Targeting the undruggable target. *Crit. Rev. Oncol. Hematol.* **92**, 107–122 (2014).
23. Johnson, D. B. *et al.* Acquired BRAF inhibitor resistance: A multicenter meta-analysis of the spectrum and frequencies, clinical behaviour, and phenotypic associations of resistance mechanisms. *Eur. J. Cancer* **51**, 2792–2799 (2015).
24. Long, G. V. *et al.* Dabrafenib plus trametinib versus dabrafenib monotherapy in patients with metastatic BRAF V600E/ K-mutant melanoma: Long-term survival

- and safety analysis of a phase 3 study. *Ann. Oncol.* **28**, 1631–1639 (2017).
25. Long, G. V. *et al.* Combined BRAF and MEK inhibition versus BRAF inhibition alone in melanoma. *N. Engl. J. Med.* **371**, 1877–1888 (2014).
 26. Rizos, H. *et al.* BRAF Inhibitor Resistance Mechanisms in Metastatic Melanoma : Spectrum and Clinical Impact. *Clin. Cancer Res.* **20**, 1965–1978 (2014).
 27. Kohl, N. E. *et al.* Protein farnesyltransferase inhibitors block the growth of ras-dependent tumors in nude mice. *Proc. Natl. Acad. Sci. U. S. A.* (1994) doi:10.1073/pnas.91.19.9141.
 28. Gajewski, T. F. *et al.* Phase II study of the farnesyltransferase inhibitor R115777 in advanced melanoma (CALGB 500104). *J. Transl. Med.* (2012) doi:10.1186/1479-5876-10-246.
 29. Moreira, R. S., Bicker, J., Musicco, F., Persichetti, A. & Pereira, A. M. P. T. Anti-PD-1 immunotherapy in advanced metastatic melanoma: State of the art and future challenges. *Life Sci.* **240**, 117093 (2020).
 30. Atkins, M. B. *et al.* High-dose recombinant interleukin 2 therapy for patients with metastatic melanoma: Analysis of 270 patients treated between 1985 and 1993. *J. Clin. Oncol.* (1999) doi:10.1200/jco.1999.17.7.2105.
 31. Hodi, F. S. *et al.* Improved survival with ipilimumab in patients with metastatic melanoma. *N. Engl. J. Med.* (2010) doi:10.1056/NEJMoa1003466.
 32. Robert, C. *et al.* Ipilimumab plus dacarbazine for previously untreated metastatic melanoma. *N. Engl. J. Med.* (2011) doi:10.1056/NEJMoa1104621.
 33. Larkin, J. *et al.* Overall survival in patients with advanced melanoma who received nivolumab versus investigator’s choice chemotherapy in CheckMate 037: A Randomized, Controlled, Open-Label Phase III Trial. *J. Clin. Oncol.* **36**, 383–390 (2018).
 34. Larkin, J. *et al.* Combined nivolumab and ipilimumab or monotherapy in untreated Melanoma. *N. Engl. J. Med.* **373**, 23–34 (2015).
 35. Larkin, J. *et al.* Five-year survival with combined nivolumab and ipilimumab in advanced melanoma. *N. Engl. J. Med.* **381**, 1535–1546 (2019).

36. Kwok, G., Yau, T. C. C., Chiu, J. W., Tse, E. & Kwong, Y. L. Pembrolizumab (Keytruda). *Hum. Vaccines Immunother.* **12**, 2777–2789 (2016).
37. Johnson, D. B. *et al.* Impact of NRAS mutations for patients with advanced melanoma treated with immune therapies. *Cancer Immunol. Res.* **3**, 288–295 (2015).
38. Kirchberger, M. C. *et al.* MEK inhibition may increase survival of NRAS-mutated melanoma patients treated with checkpoint blockade: Results of a retrospective multicentre analysis of 364 patients. *Eur. J. Cancer* (2018) doi:10.1016/j.ejca.2018.04.010.
39. Dummer, R. *et al.* Binimetinib versus dacarbazine in patients with advanced NRAS-mutant melanoma (NEMO): a multicentre, open-label, randomised, phase 3 trial. *Lancet Oncol.* **18**, 435–445 (2017).
40. Echevarría-Vargas, I. M. *et al.* Co-targeting BET and MEK as salvage therapy for MAPK and checkpoint inhibitor-resistant melanoma. *EMBO Mol. Med.* **10**, (2018).
41. Najem, A. *et al.* P53 and MITF/Bcl-2 identified as key pathways in the acquired resistance of NRAS-mutant melanoma to MEK inhibition. *Eur. J. Cancer* (2017) doi:10.1016/j.ejca.2017.06.033.
42. Reyes-Uribe, P. *et al.* Exploiting TERT dependency as a therapeutic strategy for NRAS-mutant melanoma. *Oncogene* (2018) doi:10.1038/s41388-018-0247-7.
43. Haarberg, H. E. *et al.* Inhibition of Wee1, AKT, and CDK4 underlies the efficacy of the HSP90 inhibitor XL888 in an In Vivo model of NRAS-mutant melanoma. *Mol. Cancer Ther.* (2013) doi:10.1158/1535-7163.MCT-12-1003.
44. Bertoli, E., Giavarra, M., Vitale, M. G. & Minisini, A. M. Neuroblastoma rat sarcoma mutated melanoma: That's what we got so far. *Pigment Cell Melanoma Res.* **32**, 744–752 (2019).
45. Lawrence, M. S. *et al.* Mutational heterogeneity in cancer and the search for new cancer-associated genes. *Nature* **499**, 214–218 (2013).
46. Xia, J. *et al.* A meta-analysis of somatic mutations from next generation sequencing of 241 melanomas: a road map for the study of genes with potential clinical relevance. *Mol. Cancer Ther.* **13**, 1918–28 (2014).

47. Akbani, R. *et al.* Genomic Classification of Cutaneous Melanoma. *Cell* **161**, 1681–1696 (2015).
48. Downward, J. Targeting RAS signalling pathways in cancer therapy. *Nat Rev Cancer* **3**, 11–22 (2003).
49. Samatar, A. A. & Poulidakos, P. I. Targeting RAS-ERK signalling in cancer: Promises and challenges. *Nat. Rev. Drug Discov.* **13**, 928–942 (2014).
50. Castellano, E. & Downward, J. Ras interaction with PI3K: More than just another effector pathway. *Genes and Cancer* (2011) doi:10.1177/1947601911408079.
51. Paluncic, J. *et al.* Roads to melanoma: Key pathways and emerging players in melanoma progression and oncogenic signaling. *Biochim. Biophys. Acta - Mol. Cell Res.* **1863**, 770–784 (2016).
52. Shtivelman, E. *et al.* Pathways and therapeutic targets in melanoma. *Oncotarget* **5**, 1701–1752 (2014).
53. Li, S., Balmain, A. & Counter, C. M. A model for RAS mutation patterns in cancers: finding the sweet spot. *Nat. Rev. Cancer* **18**, 767–777 (2018).
54. Dumaz, N. *et al.* Atypical BRAF and NRAS mutations in mucosal melanoma. *Cancers (Basel)*. **11**, (2019).
55. Prior, I. A., Lewis, P. D. & Mattos, C. A comprehensive survey of ras mutations in cancer. *Cancer Res.* **72**, 2457–2467 (2012).
56. Ihle, N. T. *et al.* Effect of KRAS oncogene substitutions on protein behavior: Implications for signaling and clinical outcome. *J. Natl. Cancer Inst.* **104**, 228–239 (2012).
57. De Roock, W. *et al.* Association of KRAS p.G13D Mutation With Outcome in Patients With Chemotherapy-Refractory Metastatic Colorectal Cancer Treated With Cetuximab. *JAMA* **304**, 1812–1820 (2010).
58. Burd, C. E. *et al.* Mutation-specific RAS oncogenicity explains NRAS codon 61 selection in melanoma. *Cancer Discov.* **4**, 1418–1429 (2014).
59. Jakob, J. A. *et al.* NRAS mutation status is an independent prognostic factor in metastatic melanoma. *Cancer* **118**, 4014–4023 (2012).

60. Devitt, B. *et al.* Clinical outcome and pathological features associated with NRAS mutation in cutaneous melanoma. *Pigment Cell Melanoma Res.* **24**, 666–672 (2011).
61. Tormanen, V. T. & Pfeifer, G. P. Mapping of UV photoproducts within ras proto-oncogenes in UV-irradiated cells: Correlation with mutations in human skin cancer. *Oncogene* (1992).
62. D’Adda Di Fagagna, F. *et al.* A DNA damage checkpoint response in telomere-initiated senescence. *Nature* (2003) doi:10.1038/nature02118.
63. Herbig, U., Jobling, W. A., Chen, B. P. C., Chen, D. J. & Sedivy, J. M. Telomere shortening triggers senescence of human cells through a pathway involving ATM, p53, and p21CIP1, but not p16INK4a. *Mol. Cell* (2004) doi:10.1016/S1097-2765(04)00256-4.
64. Serrano, M., Lin, A. W., McCurrach, M. E., Beach, D. & Lowe, S. W. Oncogenic ras provokes premature cell senescence associated with accumulation of p53 and p16(INK4a). *Cell* (1997) doi:10.1016/S0092-8674(00)81902-9.
65. Di Micco, R., Fumagalli, M. & d’Adda di Fagagna, F. Breaking news: high-speed race ends in arrest - how oncogenes induce senescence. *Trends in Cell Biology* (2007) doi:10.1016/j.tcb.2007.07.012.
66. Collado, M. *et al.* Tumour biology: Senescence in premalignant tumours. *Nature* **436**, 642 (2005).
67. Gorgoulis, V. *et al.* Cellular Senescence: Defining a Path Forward. *Cell* **179**, 813–827 (2019).
68. Narita, Masashi. Rb-Mediated Heterochromatin Formation and Silencing of E2F Target Genes during Cellular Senescence State University of New York at Stony Brook. **113**, 703–716 (2003).
69. Mallette, F. A., Gaumont-Leclerc, M. F. & Ferbeyre, G. The DNA damage signaling pathway is a critical mediator of oncogene-induced senescence. *Genes Dev.* (2007) doi:10.1101/gad.1487307.
70. Roos, W. P., Thomas, A. D. & Kaina, B. DNA damage and the balance between survival and death in cancer biology. *Nat. Rev. Cancer* **16**, 20–33 (2016).

71. Moiseeva, O., Mallette, F. A., Mukhopadhyay, U. K., Moores, A. & Ferbeyre, G. DNA damage signaling and p53-dependent senescence after prolonged β -interferon stimulation. *Mol. Biol. Cell* (2006) doi:10.1091/mbc.E05-09-0858.
72. Vijayachandra, K., Lee, J. & Glick, A. B. Smad3 regulates senescence and malignant conversion in a mouse multistage skin carcinogenesis model. *Cancer Res.* (2003).
73. Katakura, Y., Nakata, E., Miura, T. & Shirahata, S. Transforming growth factor β triggers two independent-senescence programs in cancer cells. *Biochem. Biophys. Res. Commun.* (1999) doi:10.1006/bbrc.1999.0129.
74. Kuilman, T. & Peeper, D. S. Senescence-messaging secretome: SMS-ing cellular stress. *Nature Reviews Cancer* vol. 9 81–94 (2009).
75. Coppé, J.-P., Desprez, P.-Y., Krtolica, A. & Campisi, J. The Senescence-Associated Secretory Phenotype: The Dark Side of Tumor Suppression. *Annu. Rev. Pathol. Mech. Dis.* **5**, 99–118 (2010).
76. Land, H., Parada, L. F. & Weinberg, R. A. Tumorigenic conversion of primary embryo fibroblasts requires at least two cooperating oncogenes. *Nature* **304**, 596–602 (1983).
77. Der, C. J., Krontiris, T. G. & Cooper, G. M. Transforming genes of human bladder and lung carcinoma cell lines are homologous to the ras genes of Harvey and Kirsten sarcoma viruses. *Proc. Natl. Acad. Sci.* **79**, 3637–3640 (1982).
78. Grivennikov, S. I. & Karin, M. Inflammation and oncogenesis: a vicious connection. *Curr. Opin. Genet. Dev.* **20**, 65–71 (2010).
79. Taniguchi, K. & Karin, M. NF- κ B, inflammation, immunity and cancer: Coming of age. *Nat. Rev. Immunol.* **18**, 309–324 (2018).
80. Korniluk, A., Koper, O., Kemonia, H. & Dymicka-Piekarska, V. From inflammation to cancer. *Ir. J. Med. Sci.* **186**, 57–62 (2017).
81. Yu, H., Pardoll, D. & Jove, R. STATs in cancer inflammation and immunity: A leading role for STAT3. *Nature Reviews Cancer* vol. 9 798–809 (2009).
82. Xiong, A., Yang, Z., Shen, Y., Zhou, J. & Shen, Q. Transcription factor STAT3 as a novel molecular target for cancer prevention. *Cancers (Basel)*. **6**, 926–957 (2014).

83. Bromberg, J. F. *et al.* Stat3 as an Oncogene. *Cell* **98**, 295–303 (1999).
84. Gupta, P. B. *et al.* The melanocyte differentiation program predisposes to metastasis after neoplastic transformation. *Nat. Genet.* **37**, 1047–1054 (2005).
85. Garraway, L. A. *et al.* Integrative genomic analyses identify MITF as a lineage survival oncogene amplified in malignant melanoma. *Nature* **436**, 117–122 (2005).
86. Bagga, M., Kaur, A., Westermarck, J. & Abankwa, D. ColonyArea : An ImageJ Plugin to Automatically Quantify Colony Formation in Clonogenic Assays. **9**, 14–17 (2014).
87. Dimri, G. P. *et al.* A biomarker that identifies senescent human cells in culture and in aging skin in vivo. *Proc. Natl. Acad. Sci.* **92**, 9363–9367 (1995).
88. Ohanna, M. *et al.* Secretome from senescent melanoma engages the STAT3 pathway to favor reprogramming of naive melanoma towards a tumor-initiating cell phenotype. *Oncotarget* **4**, 2212–2224 (2013).
89. Steingrímsson, E., Copeland, N. G. & Jenkins, N. A. Melanocytes and the Microphthalmia Transcription Factor Network . *Annu. Rev. Genet.* **38**, 365–411 (2004).
90. Tachibana, M. *et al.* Ectopic expression of MITF, a gene for Waardenburg syndrome type 2, converts fibroblasts to cells with melanocyte characteristics. *Nat. Genet.* **14**, 50–54 (1996).
91. Goding, C. R. & Arnheiter, H. MITF — the first 25 years. 983–1007 (2019) doi:10.1101/gad.324657.119.ness.
92. Müller, J. *et al.* Low MITF/AXL ratio predicts early resistance to multiple targeted drugs in melanoma. *Nat. Commun.* **5**, (2014).
93. Sensi, M. *et al.* Human cutaneous melanomas lacking MITF and melanocyte differentiation antigens express a functional Axl receptor kinase. *J. Invest. Dermatol.* **131**, 2448–2457 (2011).
94. Wang, M., Tan, Z., Zhang, R., Kotenko, S. V. & Liang, P. Interleukin 24 (MDA-7/MOB-5) signals through two heterodimeric receptors, IL-22R1/IL-20R2 and IL-20R1/IL-20R2. *J. Biol. Chem.* **277**, 7341–7347 (2002).

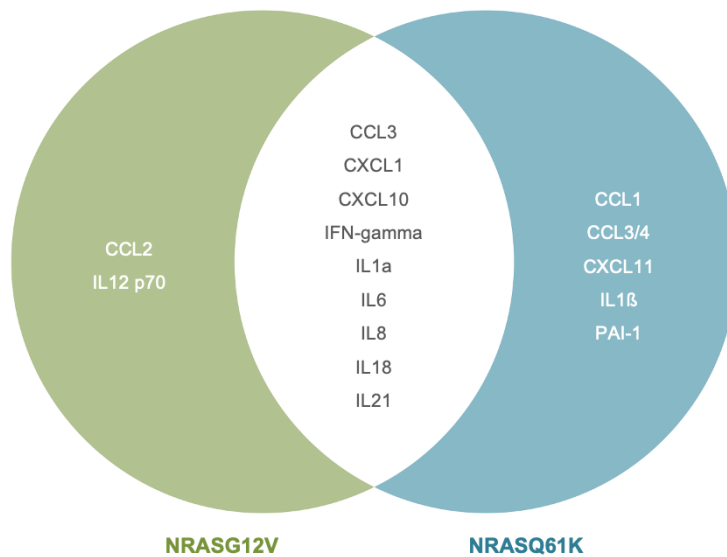
95. Novakova, Z. *et al.* Cytokine expression and signaling in drug-induced cellular senescence. *Oncogene* **29**, 273–284 (2010).
96. Shain, A. H. *et al.* The Genetic Evolution of Melanoma from Precursor Lesions. *N. Engl. J. Med.* **373**, 1926–1936 (2015).
97. Hanahan, D. & Weinberg, R. A. Hallmarks of cancer: The next generation. *Cell* **144**, 646–674 (2011).
98. Haigis, K. M. *et al.* Differential effects of oncogenic K-Ras and N-Ras on proliferation, differentiation and tumor progression in the colon. *Nat. Genet.* **40**, 600–608 (2008).
99. De Roock, W. *et al.* Association of KRAS p.G13D Mutation With Outcome in Patients With Chemotherapy-Refractory Metastatic Colorectal Cancer Treated With Cetuximab. *JAMA* **304**, 1812–1820 (2010).
100. Bauer, J., Curtin, J. A., Pinkel, D. & Bastian, B. C. Congenital melanocytic nevi frequently harbor NRAS mutations but no BRAF mutations. *J. Invest. Dermatol.* **127**, 179–182 (2007).
101. Tschandl, P. *et al.* NRAS and BRAF Mutations in Melanoma-Associated Nevi and Uninvolved Nevi. *PLoS One* **8**, 1–8 (2013).
102. Pampena, R. *et al.* A meta-analysis of nevus-associated melanoma: Prevalence and practical implications. *J. Am. Acad. Dermatol.* **77**, 938-945.e4 (2017).
103. Kakavand, H. *et al.* Concordant BRAFV600E mutation status in primary melanomas and associated naevi: Implications for mutation testing of primary melanomas. *Pathology* **46**, 193–198 (2014).
104. Shitara, D. *et al.* Mutational status of naevus-associated melanomas. *Br. J. Dermatol.* **173**, 671–680 (2015).
105. Shain, A. H. & Bastian, B. C. From melanocytes to melanomas. *Nat. Rev. Cancer* **16**, 345–358 (2016).
106. Posch, C. *et al.* Phosphoproteomic Analyses of NRAS(G12) and NRAS(Q61) Mutant Melanocytes Reveal Increased CK2?? Kinase Levels in NRAS(Q61) Mutant Cells. *J. Invest. Dermatol.* (2016) doi:10.1016/j.jid.2016.05.098.

107. Deribe, Y. L. *et al.* Truncating PREX2 mutations activate its GEF activity and alter gene expression regulation in NRAS-mutant melanoma. *Proc. Natl. Acad. Sci. U. S. A.* **113**, E1296–E1305 (2016).
108. Kunimoto, H. *et al.* Cooperative Epigenetic Remodeling by TET2 Loss and NRAS Mutation Drives Myeloid Transformation and MEK Inhibitor Sensitivity. *Cancer Cell* **33**, 44–59.e8 (2018).
109. Tellez, C. S. *et al.* CpG island methylation profiling in human melanoma cell lines. *Melanoma Res.* **19**, 146–155 (2009).
110. Wang, Y. *et al.* Mutant N-RAS protects colorectal cancer cells from stress-induced apoptosis and contributes to cancer development and progression. *Cancer Discov.* **3**, 294–307 (2013).
111. Orecchia, V. *et al.* Constitutive STAT3 activation in epidermal keratinocytes enhances cell clonogenicity and favours spontaneous immortalization by opposing differentiation and senescence checkpoints. *Exp. Dermatol.* **24**, 29–34 (2015).
112. Fedorenko, I. V. *et al.* Phosphoproteomic analysis of basal and therapy-induced adaptive signaling networks in BRAF and NRAS mutant melanoma. *Proteomics* **15**, 327–339 (2015).
113. Mandal, T. *et al.* Reduced phosphorylation of Stat3 at Ser-727 mediated by casein kinase 2 - Protein phosphatase 2A enhances Stat3 Tyr-705 induced tumorigenic potential of glioma cells. *Cell. Signal.* **26**, 1725–1734 (2014).
114. Xu, L. *et al.* IGF1/IGF1R/STAT3 signaling-inducible IFITM2 promotes gastric cancer growth and metastasis. *Cancer Lett.* **393**, 76–85 (2017).
115. Paccez, J. D. *et al.* The receptor tyrosine kinase Axl is an essential regulator of prostate cancer proliferation and tumor growth and represents a new therapeutic target. *Oncogene* **32**, 689–698 (2013).
116. Xie, T. X. *et al.* Activation of Stat3 in human melanoma promotes brain metastasis. *Cancer Res.* **66**, 3188–3196 (2006).
117. Rotte, A., Martinka, M. & Li, G. MMP2 expression is a prognostic marker for primary melanoma patients. *Cell. Oncol.* **35**, 207–216 (2012).

118. da Silva, W. C. *et al.* Genotyping and differential expression analysis of inflammasome genes in sporadic malignant melanoma reveal novel contribution of CARD8, IL1B and IL18 in melanoma susceptibility and progression. *Cancer Genet.* **209**, 474–480 (2016).
119. Okamoto, M. *et al.* Constitutively active inflammasome in human melanoma cells mediating autoinflammation via caspase-1 processing and secretion of interleukin-1 β . *J. Biol. Chem.* **285**, 6477–6488 (2010).
120. Bowman, T. *et al.* Stat3-mediated Myc expression is required for Src transformation and PDGF-induced mitogenesis. *Proc. Natl. Acad. Sci.* **98**, 7319–7324 (2001).
121. Chiariello, M., Marinissen, M. J. & Gutkind, J. S. Regulation of c-myc expression by PDGF through Rho GTPases. *Nat. Cell Biol.* **3**, 580–586 (2001).
122. Kolligs, F. T. *et al.* γ -Catenin is regulated by the APC tumor suppressor and its oncogenic activity is distinct from that of β -catenin. *Genes Dev.* **14**, 1319–1331 (2000).
123. Zhuang, D. *et al.* C-MYC overexpression is required for continuous suppression of oncogene-induced senescence in melanoma cells. *Oncogene* **27**, 6623–6634 (2008).
124. Pelengaris, S., Khan, M. & Evan, G. c-MYC: More than just a matter of life and death. *Nat. Rev. Cancer* **2**, 764–776 (2002).
125. Kortylewski, M., Jove, R. & Yu, H. Targeting STAT3 affects melanoma on multiple fronts. *Cancer and Metastasis Reviews* vol. 24 315–327 (2005).
126. Furtek, S. L., Backos, D. S., Matheson, C. J. & Reigan, P. Strategies and Approaches of Targeting STAT3 for Cancer Treatment. *ACS Chemical Biology* vol. 11 308–318 (2016).
127. Furqan, M., Akinleye, A., Mukhi, N., Mittal, V., Chen, Y., & Liu, D. STAT inhibitors for cancer therapy. *J Hematol Oncol.* **6**, 1–11 (2013).
128. Kim, Y. *et al.* AZD9150, a next-generation antisense oligonucleotide inhibitor of STAT3 with early evidence of clinical activity in lymphoma and lung cancer . *Sci. Transl. Med.* **7**, 314ra185-314ra185 (2015).

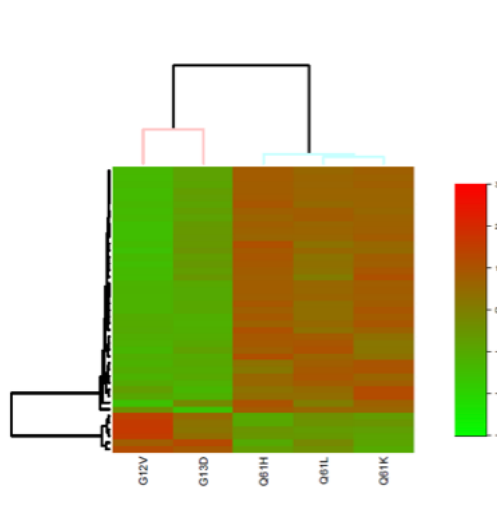
7 SUPPLEMENTARY FIGURES AND TABLES

7.1 Supplementary Figures



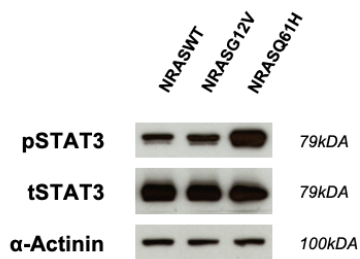
Supplementary Figure 1 | Upregulated cytokines in *NRAS* mutants

Upregulated cytokines of *NRASG12V* and *NRASQ61K* expressing NHM compared to *NRAS* wildtype and empty vector.



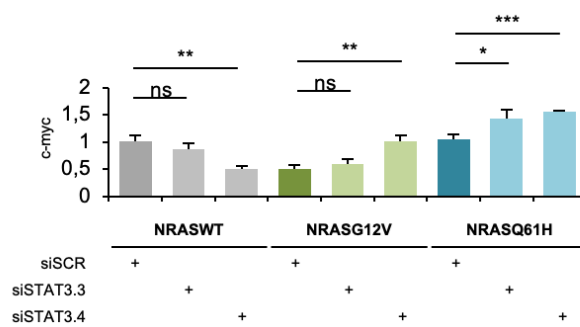
Supplementary Figure 2 | Gene expression profiling shows 43 differentially deregulated genes in NHM

Microarray Analysis and clustering of cell lines expressing either *NRASG12/13* or *NRASQ61* shows 43 regulated genes.



Supplementary Figure 3 | *NRASQ61H* activates STAT3

Western Blot Analysis of phosphorylated STAT3 shows higher activation of STAT3-signaling in *NRASQ61H* expressing MelSTV.



Supplementary Figure 4 | Knockdown of STAT3 upregulates c-myc in MelSTV

mRNA expression of *c-myc* is increased after 48 hours transfection with siSTAT3. Data normalized to *NRASWT* siSCR and shown as fold change. ns=not significant * $p < 0.05$ ** $p < 0.01$ *** $p < 0.001$

7.2 Supplementary Tables

7.2.1 Supplementary Table 1

Name	Gene	adjusted P-value	Fold Change
TAGLN3	<i>transgelin 3</i>	0.000121	1,1050
SERPINB2	<i>serpin peptidase inhibitor, clade B (ovalbumin), member 2</i>	0.000752	1,0867
BEX1	<i>brain expressed, X-linked 1</i>	0.001452	1,0350
STC1	<i>stanniocalcin 1</i>	0.000333	1,0050
ANGPTL4	<i>angiopoietin-like 4</i>	1.8e-05	0,9983
IL1B	<i>interleukin 1, beta</i>	1.8e-05	0,9700
RAC2	<i>ras-related C3 botulinum toxin substrate 2 (rho family, small GTP binding protein Rac2)</i>	3.8e-05	0,9700
VGF	<i>VGF nerve growth factor inducible</i>	0.044913	0,9250
IL24	<i>interleukin 24</i>	3.8e-05	0,8700
CXCL8	<i>chemokine (C-X-C motif) ligand 8</i>	0.008998	0,8400
TMEM158	<i>transmembrane protein 158 (gene/pseudogene)</i>	0.000129	0,8367
ERRFI1	<i>ERBB receptor feedback inhibitor 1</i>	7.7e-05	0,8333

AXL	<i>AXL receptor tyrosine kinase</i>	0.003171	0,7867
NRP1	<i>neuropilin 1</i>	0.001997	0,7583
GPAT3	<i>glycerol-3-phosphate acyltransferase 3</i>	0.002515	0,7533
MMP1	<i>matrix metalloproteinase 1</i>	0.002234	0,7067
IL13RA2	<i>interleukin 13 receptor, alpha 2</i>	0.002515	0,6783
SLC20A1	<i>solute carrier family 20 (phosphate transporter), member 1</i>	0.001298	0,6767
FAM19A3	<i>family with sequence similarity 19 (chemokine (C-C motif)-like), member A3</i>	0.002515	0,6700
DDIT4	<i>DNA-damage-inducible transcript 4</i>	0.002067	0,6417
CLCF1	<i>cardiotrophin-like cytokine factor 1</i>	0.001375	0,6133
OCIAD2	<i>OCIA domain containing 2</i>	0.00285	0,5883
TAGLN3	<i>transgelin 3</i>	0.005352	0,5850
ERCC1	<i>excision repair cross- complementation group 1</i>	0.00285	0,5817
TFPI2	<i>tissue factor pathway inhibitor 2</i>	0.008609	0,5817
CYB5R2	<i>cytochrome b5 reductase 2</i>	0.005849	0,5667

8 CURRICULUM VITAE

JAMES KIM

29.05.1994 in Heidelberg

EDUCATION

OCTOBER 2012 – DECEMBER 2019	University of Heidelberg (Medical Faculty Mannheim) Medicine 1 st part of the National Medical Licensing Exam: Grade 1.0 2 nd part of the National Medical Licensing Exam: Grade 2.0 3 rd part of the National Medical Licensing Exam: Grade 1.0
AUGUST 2016 – JANUARY 2020	German Cancer Research Center (DKFZ) Heidelberg Dissertation to obtain the Doctor of Medicine (M.D.) degree Title: <i>STAT3 – Mediator of differential cellular and molecular responses to melanoma associated NRAS mutations</i>
AUGUST 2016 – JANUARY 2020	RTG 2099 - Hallmarks of Skin Cancer Member and doctoral scholarship of the graduate college
FEBRUARY 2015 – JULY 2015	Junior Scientific Master Class 2015 Introduction Course, Scientific Writing, Presentation Skills, Laboratory Courses, Biostatistics
OCTOBER 2013	Elective at the University of Heidelberg Translational Medical Research Grade: 1.0
SEPTEMBER 2004 – JUNE 2012	Kant-Gymnasium Karlsruhe General qualification for university entrance (Abitur) Average grade: 1.0

PUBLICATIONS

Kim, Novak, Sachpekidis, Utikal & Larribère. STAT3 Relays a Differential Response to Melanoma-Associated NRAS Mutations. *Cancers (Basel)*. **12**, 119 (2020).

9 ACKNOWLEDGEMENTS

Writing these last lines of my dissertation, I realize that this whole process was the result of a long journey. It made me grow not only in scientific matters, but also personally and in broadness and openness towards unexpected events through the inputs from very precious colleagues in the field.

This work would not have been possible without a lot of people who accompanied me during this process.

First, I want to thank *Prof. Dr. Jochen Utikal* for offering me the possibility to do research on the exciting and innovative field of *NRAS* mutations in melanoma. His supervision and clinical expertise enabled me to see the broad clinical implications when I was lost on the cell level.

Special thanks also go to *Dr. Lionel Larribère* in whose preparatory work I could directly dive into. He supported me from scratch in the practical work at the bench with his scientific inputs and discussions as well as in the finalization of the work and in the publication and writing of this thesis. He was always available when I needed support. Not only as a mentor, but also as a friend, I truly enjoyed my stay at the DKFZ.

Thank you, *Laura*, for your assistance in the laboratory work and your corrections and suggestions for my thesis.

What would the bench be without great colleagues? I want to thank *Daniel, Sachindra, Huizi, Karol, Laura, Nello* and *Sunee* for the great team spirit and the joyful and funny moments which made the start into lab work much more colorful. I made new friends which I am very grateful for. Moreover, I am happy to have gotten to know *Tamara, Juliane, Marlene, Ke* and *Ze* who joined later: It was a pleasure working with you!

Jenny! I thank you for all the technical support in the laboratory and your expertise and the exciting off topic discussions.

I am thankful for having been part of *RTG 2099 Hallmarks of Skin Cancer*. Not only the financial support, but also the whole scientific program and the broad network it offered completed the full experience.

Furthermore, I am glad that I have been able to work at the *German Cancer Research Center (DKFZ)*. The great facility with its powerful infrastructure and possibilities made research truly enjoyable. I thank the microarray unit of the *DKFZ Genomics and Proteomics Core Facility* for providing the Illumina Whole-Genome Expression Beadchips and related services.

Last but not least, I want to express my deep thankfulness to my family. They supported me in every situation with their full understanding and love.

Turning this last page, I finish a big chapter which would not have been possible without each one of you. But it certainly was not the last and will encourage me to go through much more in the future.